

SCG060-01

Room:302

Time:May 25 08:30-08:45

Towards mapping of geofluids

Hikaru Iwamori^{1*}, Tohru Watanabe², Michihiko Nakamura³, Masahiro Ichiki³, Junichi Nakajima³

¹Tokyo Institute of Technology, ²Toyama University, ³Tohoku University

There are accumulating evidences indicating that geofluids in subduction zones play important roles in various phenomena, such as seismic and magmatic activities, crustal deformation, metamorphism, evolution of continental crust, and global material differentiation. However, in situ distribution of geofluids within the crust and the mantle, or even their presence, has not been identified with sufficient resolution, hence their roles in the various phenomena mentioned above remain unclear.

Low seismic velocities and/or a high electrical conductivity have conventionally been regarded as diagnostic features for presence of geofluids (e.g., Nakajima and Hasegawa, 2003). Overlapping thermal, compositional and textural variations blur the features specific to geofluids, and the number of unknown parameters apparently exceeds the number of observed variables (e.g., Watanabe, 2005). Therefore, introducing a priori information and models (e.g., thermal and petrological structures) into the analysis (i.e., deducing phase, fraction, geometry [represented by, e.g., aspect ratio] and their spatial distribution of geofluids based on the seismic velocity and electrical conductivity) is necessary. In addition, some key variable or parameter could be sensitive enough to constrain a parameter for geofluids beyond the background variations, eliminating uncertainties introduced by a priori information and models. In this paper, we discuss both aspects, i.e., (i) integration of available information, and (ii) key variables or parameters sensitive to geofluids.

In order to quantitatively identify the spatial distribution of geofluids, we combine (1) observed seismic velocity structure, (2) observed electrical conductivity structure, (3) petrological model, and (4) thermal model, for areas with well-resolved tomography of both seismic velocity and electrical conductivity. The models of (3) and (4) correspond to the point (i) above. Concerning the point (ii), we focus on the contrast between (1) and (2): for a typical case, distribution of low velocity regions coincide well with that of highly conductive regions (e.g., those beneath the northern Miyagi Prefecture area [Mitsuhashi et al., 2001; Nakajima and Hasegawa, 2003]), associated with a few percent decrease in the seismic velocity and two to four orders of magnitude increase in the electrical conductivity. Inspection of all the plausible factors strongly suggests that the huge contrast in amplitude between the seismic velocity and the electrical conductivity may be resolved only when a variation of fluid fraction affects linearly the seismic velocity and nonlinearly the electrical conductivity.

This differential response may arise from the fact that the seismic velocity is approximately a linear function of fluid fraction (Takei, 2002) and is insensitive to the connectivity, whereas the electrical conductivity is sensitive to the connectivity. If the connectivity of fluid increases with its volume fraction, this causes a nonlinear increase of electrical conductivity with the fluid fraction. We thus think that the relationship between connectivity and fluid fraction is a key to interpret the observed seismic velocity and electrical conductivity. Deciphering this relationship, being combined with thermal and petrological models, could be a useful and robust approach to map geofluid distribution.

Japan Geoscience Union Meeting 2011

(May 22-27 2011 at Makuhari, Chiba, Japan)

©2011. Japan Geoscience Union. All Rights Reserved.



SCG060-02

Room:302

Time:May 25 08:45-09:00

Pb isotopic compositions of hydrothermal deposits in the Japanese island arc as a tracer of slab-fluids

Koichiro Fujinaga^{1*}, Yasuhiro Kato¹, Yutaro Takaya¹, Masaharu Tanimizu², Hikaru Iwamori³

¹University of Tokyo, ²JAMSTEC, ³Tokyo Institute of Technology

Quite recently, it has been pointed out that "geofluids" released from the subducting plates may be involved in various phenomena in subduction zone, such as young volcanic rocks, deep-seated hot springs and hydrothermal deposits. Systematical investigations of these various materials are needed for identifying the geochemical characteristics of the geofluids. Nakamura et al. (2008) revealed that the slab-fluids derived from two subducted plates (the Pacific plate and the Philippine Sea plate) contribute largely to the genesis of arc magmas in the Central Japan. Here we focus on hydrothermal deposits (vein-type and skarn-type) in the Japanese island arc. Hydrothermal fluids that formed sulphide mineral (galena, pyrite, chalcopyrite, sphalerite etc.) deposits are generally considered to have been derived from magmatic and/or meteoric waters based on H, C, O, and S isotopes in the deposit materials. However, ore fluids may be directly derived from deep fluids. We report Pb isotopic compositions of hydrothermal deposits in the Central Japan and discuss about the origin of ore fluids.

SCG060-03

Room:302

Time:May 25 09:00-09:15

Slab-Derived Halogens and Noble Gases Preserved in Peridotite and Eclogite from the Sanbagawa Metamorphic Belt

Hirochika Sumino^{1*}, Shunsuke Endo², Kenta Yoshida³, Tomoyuki Mizukami⁴, Simon Wallis², Takao Hirajima³, Ray Burgess⁵, Chris Ballentine⁵

¹GCRC, University of Tokyo, ²Nagoya University, ³Kyoto University, ⁴Kanazawa University, ⁵SEAES, University of Manchester

Subduction volcanism is generally considered to form a 'subduction barrier' that efficiently recycles volatile components contained in subducted slabs back to the Earth's surface (Staudacher and Allegre, 1988, *Earth Planet. Sci. Lett.* 89, 173-183). Nevertheless, subduction of sediment and seawater-dominated pore fluids to the deep mantle has been proposed to account for heavy noble gas (Ar, Kr and Xe) non-radiogenic elemental abundance and isotopic pattern of the convecting mantle (Holland and Ballentine, 2006, *Nature* 441, 186-191). To verify whether and how subduction fluids preserve a seawater signature, we have determined noble gas and halogen compositions of the Higashi-akaishi peridotite and Western Iratsu and Seba eclogite bodies in the Sanbagawa metamorphic belt, southwest Japan, in which relicts of slab-derived water are contained as hydrous mineral inclusions in wedge mantle rocks exhumed from depths in excess of 100 km (Mizukami et al., 2004, *Nature* 427, 432-436) and aqueous fluid inclusions in associated slab-derived eclogites and quartz veins/lenses (Endo et al., 2009, *J. Metamorphic Geol.* 27, 371-384; Endo, 2010, *Isl. Arc* 19, 313-335; Hirajima et al., 2010, *Geophys. Res. Abst.* 12, EGU2010-6343).

The striking similarities of the observed noble gas and halogen compositions of the Higashi-akaishi peridotite with marine pore fluids (Sumino et al., 2010, *Earth Planet. Sci. Lett.* 294, 163-172) challenge a popular concept, in which the water flux into the mantle wedge is only by hydrous minerals in altered oceanic crust and sediment (e.g., Schmidt and Poli, 1998, *Earth Planet. Sci. Lett.* 163, 361-379). The Western Iratsu eclogite also exhibits non-radiogenic noble gas and halogen elemental ratios well explained by a mixing between seawater-derived and sedimentary components. These results indicate that subduction and closed system retention of marine pore fluid occurs up to depths of at least 100 km. Two mechanisms of subduction of unfractionated pore fluid-derived noble gas and halogens are proposed: one is that a portion of pore-fluid in sediments and/or crust subducts to a depth deeper than the overlying crust and is liberated and incorporated into grain boundaries of the mantle peridotite that is dragged down by flow in the mantle along with the downgoing slab. The other is that hydrated lithospheric mantle, resulting from penetration of pore-fluid along bending-related faulting of the oceanic plate entering subduction zones, preserves unfractionated noble gases and halogens of pore-fluid origin and transports them to the deep mantle.

The subducted halogen and noble gas compositions are clearly distinct from those of arc volcanic gases. This implies that the subduction-related metamorphic rocks of the Sanbagawa belt appear to have frozen-in and preserved a previously unseen part of the deep water recycling process whereby noble gases and halogens (and probably other volatiles) are injected into the wedge mantle just above the subducting slab, requiring a reassessment of the dominant transport mechanism and source of water in subduction zones. A small proportion of marine pore fluid, preserved in the downgoing hydrous peridotite and/or eclogite, can account for the heavy noble gas composition observed in the convecting mantle.

Keywords: noble gas, halogen, fluid inclusion, slab fluid, subduction zone, mantle wedge

SCG060-04

Room:302

Time:May 25 09:15-09:30

Metamorphic fluid composition determined by trace element and isotopic composition analysis of metamorphic rocks

Masaaki Uno^{1*}, Hikaru Iwamori¹, Hitomi Nakamura¹, Kenta Ueki¹, Taeho Park¹, Tetsuya Yokoyama¹, Masaharu Tanimizu²

¹Tokyo Institute of Technology, ²JAMSTEC

Regional metamorphic belts provide unique information that is directly relevant to the fluid behavior at plate convergent margin. Petrological and geochemical analyses of the regional metamorphic rocks would resolve not only the composition and amount of geofluids in subduction zones, which can be assessed by those of arc volcanic rocks, but also the transport mechanism of geofluids through quantification of fluid-related textures. However, previous studies on composition, amount, transport-scale of geofluids during metamorphism are inconsistent with each other (e.g. Ferry, 1992; Bebout, 2007). Although the bulk composition of metamorphic rocks represents integration of processes from subduction to exhumation, previous studies did not decode the processes, including sea floor alteration, dehydration and rehydration during subduction, which likely resulted in misinterpretations. Rehydration reaction, in particular, overprints the other two processes (e.g. Okamoto&Toriumi, 2005). In order to understand the fluid processes relevant to metamorphism, it is, therefore, required to identify and separate the processes and the associated material transport.

In this study, we aim to constrain fluid behavior in metamorphism, especially composition, amount, timing of fluid during rehydration reaction in the late stage of metamorphism by comparing geochemical data (bulk trace element and isotopic compositions, bulk water content) with petrogenetic physico-chemical conditions of P-T path, mineralogy and extent of rehydration.

The Sanbagawa metamorphic belt, a subduction-related high P/T-type regional metamorphic belt, was selected for this study, for which extensive petrogenetic information is available. For metabasaltic samples in each metamorphic grade, major and trace elements and Pb isotope analysis were conducted. Mineral composition analysis by EPMA and determination of P-T paths by thermodynamic analysis have been also performed for a part of the samples.

Consequently, we obtained the following results:

- (1) Trace element compositions of metabasites are approximately between the altered oceanic crust and oceanic sediments.
- (2) Analyzed trace elements can be divided into the following 3 groups:
 1. Elements whose concentration differs according to metamorphic grade.
 2. Elements whose concentration is proportional to bulk water (LOI).
 3. Elements which do not have trends above.
- (3) Pb isotopic compositions corrected by rehydration age are not aligned on the mixing line between AOC and sediments, but have higher $^{206}\text{Pb}/^{204}\text{Pb}$ and $^{208}\text{Pb}/^{204}\text{Pb}$ ratio.
- (4) Pb isotopic compositions of metabasites form a trend that corresponds to the IC2 components of global basalt composition proposed by Iwamori et al. (2010), which reflects hydration-dehydration process.

From samples corrected from a single basic block, a linear relationship between elements in (2)-2 and extent of rehydration was found, and fluid composition during rehydration was determined. The concentrations of each element are approximately 650, 480 and 1000 ppm for Rb, Ba and Li, respectively. The concentrations of these elements in the retrograde fluid are of an order comparable to that of fluid from subducting AOC or sediment, but they cannot be explained by linear mixing of AOC fluid and sediment fluid.

The result (4) implies that observed variation in trace element and isotope composition could reflect global differentiation common to the subduction zone fluid processes.

These results suggest that identifying mass transfer associated with rehydration process is possible, by focusing samples collected exclusively from the same basic block, whose samples are likely to have suffered the same P-T path and had a similar initial composition before subduction. A comprehensive study combining metamorphic texture, bulk trace and isotopic composition and thermodynamic analysis at Sanbagawa metamorphic belt has a potential to resolve the fluid processes in the subduction

zone.

Keywords: metamorphism, fluid, trace element, isotope, Sanbagawa metamorphic belt, Geofluid

Japan Geoscience Union Meeting 2011

(May 22-27 2011 at Makuhari, Chiba, Japan)

©2011. Japan Geoscience Union. All Rights Reserved.



SCG060-05

Room:302

Time:May 25 09:30-09:45

Effects of pressure and salinity on partitioning between magma and aqueous fluids at HTHP

Tatsuhiko Kawamoto^{1*}, Kenji Mibe², Ken'iti Kuroiwa¹, Tetsu Kogiso³

¹Inst. Geothermal Sci., Kyoto Univ., ²ERI, Univ. Tokyo, ³Human & Environment Studies, Kyoto Univ.

We will show our new experimental results to understand the effects of pressure and salinity on partitioning between a magma and aqueous fluids at high-temperature and high-pressure conditions using multi anvil apparatus at SPring-8. We will present the followings: (1) we can observe XRF spectra under high-temperature and high-pressure conditions and (2) know the effects of pressure and salinity on trace elemental partitioning between a magma and aqueous fluids, and then conclude (3) that the present data sets are not inconsistent with a previous data set based on quenched experiments by Keppler (1996, Nature). The last point suggests that slab-derived fluids are likely to be saline fluids, which can be able to dissolve significant amounts of trace elements characterizing subduction-zone magmatism.

Keywords: water, magma, high-pressure and high-temperature, elemental partition, synchrotron X-ray, subduction zone

SCG060-06

Room:302

Time:May 25 09:45-10:00

Influence of confining and pore fluid pressures on velocity and conductivity of water-saturated rock

Tohru Watanabe^{1*}, Kuno Ayumi¹, Akiyoshi Higuchi¹

¹University of Toyama

Pore fluid pressure in seismogenic zones can play a key role in the occurrence of an earthquake (e.g., Sibson, 2009). Its evaluation via seismic velocities and electrical conductivity can lead to a good understanding of seismic activities. It is essential to understand how seismic velocities and electrical conductivity reflect the pore fluid pressure. We have conducted measurements of elastic wave velocity and electrical conductivity of a water-saturated rock for various confining and pore fluid pressures.

Measurements have been made using a 200 MPa hydrostatic pressure vessel, in which the confining and pore fluid pressures can be separately controlled (Watanabe et al., 2008). Conductivity measurement requires the electrical isolation between water in a rock sample and the metal work of the pressure vessel. A plastic (PEEK) endpiece was specially designed to get electrical isolation between water in a sample and the metal work. The endpiece has a built-in plastic (DURACON) piston, which passes the pressure of oil from an external pump to the pressure of water in a sample. A good linear relationship between the oil and water pressures has been confirmed. The friction of the piston causes only 2-3% difference between oil and water pressures.

Berea sandstone was used for its high porosity (19.1%) and permeability ($3 \times 10^{-13} \text{ m}^2$). Cylindrical samples have dimension of 25 mm in diameter and 30 mm in length. Their axes are perpendicular to the sedimentation bed. The grain size is 100-200 micrometer. A dry sample has $V_p=3.2-3.3 \text{ km/s}$ and $V_s=1.9-2.0 \text{ km/s}$ in the direction perpendicular to the axis, and $V_p=3.0-3.1 \text{ km/s}$ and $V_s=1.9 \text{ km/s}$ in the direction parallel to the axis. Velocities are slightly lower in the direction perpendicular to the sedimentation bed. A water-saturated sample has $V_p=3.5 \text{ km/s}$ and $V_s=2.1 \text{ km/s}$ in the direction perpendicular to the axis. A significant increase in V_p is caused by water saturation. When the pore fluid pressure is kept constant, V_p and V_s increase with increasing confining pressure. When the confining pressure is kept constant V_p and V_s decrease with increasing pore fluid pressure. The effective confining pressure is defined by the difference between the confining and pore fluid pressures. The change in V_p and V_s shows a good correlation with the effective confining pressure. V_p and V_s increases with increasing effective confining pressure. Only a small increase is observed when the effective confining pressure is higher than 60 MPa. Similar results on Berea sandstone have been already reported by Christensen and Wang (1985). We will also report the results of electrical conductivity.

Keywords: elastic wave velocity, electrical conductivity, confining pressure, pore fluid pressure, water-saturated rock

A Bayesian approach to spatial estimation of fluid content and geometry in the mantle wedge

Tatsu Kuwatani^{1*}, Kenji Nagata¹, Masato Okada¹, Mitsuhiro Toriumi¹

¹Frontier Sci., Univ. of Tokyo

Recent development of seismic tomography enables us to image the detailed velocity structure in the mantle wedge beneath the Japanese islands (e.g. Nakajima et al., 2001). Nakajima et al. (2005) clarified the variations of porosity and pore geometry from the reduction degree of V_p and V_s data sets in the mantle wedge of the NE Japan by using the unified formulation of the effect of fluid phase on the seismic velocity. However, it is difficult to image the spatial distributions of porosity and pore geometry because seismic velocity data always have error. In this study, we try to image the porosity and pore geometry by using the Markov random field model, which is a type of Bayesian stochastic method that is often applied to image analysis. The spatial continuity of porosity and pore geometry is incorporated by Gaussian Markov Chains as prior probabilities in order to apply the MRF model to our problem. The most probable estimation can be obtained by maximizing the posterior probability of the fluid distribution given the observed velocity structures. In the present study, the steepest descent method was implemented in order to maximize the posterior probability using the Markov chain Monte Carlo (MCMC) algorithm. First, synthetic inversion tests are conducted in order to investigate the effectiveness and validity of the proposed model. Then, we apply the model to the natural data sets of the seismic velocity structures in the mantle wedge (Matsubara et al. 2008), by assuming the physical properties other than porosity and pore geometry (i.e. temperature and type of fluid) are given. Finally, we discuss the validity of the assumption and our model.

Keywords: fluid, mantle wedge, Bayesian estimation

SCG060-08

Room:302

Time:May 25 10:15-10:30

Spreadsheet mass balance for exploring on element behavior between subducted slab, mantle wedge, and magma

Jun-Ichi Kimura^{1*}, Hiroshi Kawabata¹, Bradley R. Hacke², Peter E. van Keken³, James B. Gill⁴, Robert J. Stern⁵

¹IFREE/JAMSTEC, ²University of California, Santa Barbara, ³University of Michiga, ⁴University of California Santa Cruz, ⁵University of Texas at Dallas

We have developed the Arc Basalt Simulator version 3 (ABS3), a quantitative calculator to examine the mass balance of (1) slab-dehydration and melting, and (2) slab fluid/melt-fluxed mantle melting, and to quantitatively evaluate magma genesis beneath arcs. Calculation results from the ABS3 model suggest that element re-distribution between the subducted slab and slab-derived liquid controls distinctive trace element signatures found in arc magmas and crust. The slab liquid is derived from various mixtures of fluids and melts from sediment and altered oceanic crust, dependent on the thermal structure of the subducted slab. Slab fluids are mostly generated by slab-dehydration to form the volcanic front (VF) magmas with slab P-T conditions around 3 GPa/ 750(C), whereas slab may melt at 3-6 GPa > 830(C) contributing either to the VF or to rear arc (RA) magmas. Compositions of slab fluids and melts are controlled primarily by breakdown of amphibole and lawsonite for VF and phengite for RA slab depths in association with the residual eclogite mineral phases including garnet, clinopyroxenes, and quartz. Temperature dependent partition coefficients and different partition coefficients between melt/fluid and minerals are additional controls. Minor mineral phases such as zircon and titanite also play important roles for certain elements. The slab liquid fluxed melting of depleted mantle wedge peridotite plays additional role to element re-distribution in subduction zone. The degree of partial melting varies between 17-28 % (VF) and 3-22 % (RA), with a slab flux fraction of 2-4.5 % (e.g., VF fluid) to 1-1.5 % (e.g., RA melt), and at melting depths corresponding to 1-2.5 GPa (VF) and 2.4-2.8 GPa (RA). Addition of fluid-immobile elements from the mantle contributes 78-98 % of the magma mass and controls certain isotopes such as Nd and Hf in arc magmas. However, element addition from the slab liquid modifies the liquid mobile elements/isotopes in the arc magmas significantly. The residual peridotite composition is also altered due to modification by the slab flux addition and melt depletion. Modeled peridotite compositions are similar to some peridotites in supra-subduction zone ophiolites, suggesting that element re-distribution beneath arcs is complex.

Keywords: Geochemistry, slab, mantle wedge, magma, mass balance

SCG060-09

Room:302

Time:May 25 10:45-11:00

A numerical examination of quartz precipitations from ascending fluids and resultant increases in fluid pressures

Kenichi Hoshino^{1*}, Kazuna Fujita¹

¹Grad. Sch. Sci., Hiroshima Univ.

Precipitations of quartz from ascending fluids in fractures and resultant increases in fluid pressures have been numerically simulated to examine the fault-valve model of Sibson et al. (1988) and Sibson (1992). Although a number of detailed analyses have already been made to investigate crack sealing processes around fault zones (e. g., Gratier et al., 2003), essential features of ascending fluids with mineral precipitations resulting in fracture closures have not been analyzed yet. Therefore, two simplified fluid ascending processes have been investigated in the present study: (a) fluids ascend slowly with their temperatures following geothermal gradients and (b) fluids ascend rapidly resulting in isenthalpic or semi-isenthalpic temperature decreases. It can be supposed that the natural fluid ascending systems may take the properties of between (a) and (b).

Decreasing rates of quartz solubility with decreasing temperatures and/or pressures are larger at higher temperatures and pressures. Therefore, when the fluids ascend slowly, the maximum precipitation of quartz may take place at the bottom of the fracture. The precipitation of quartz decreases the fracture width, hence raises the fluid pressure at the bottom. The consequent increase in the fluid pressure gradient may enhance the precipitation, resulting in the most rapid closure of the fracture at the bottom.

When the fluids ascend isenthalpically, boiling conditions may achieve at all depths in the fractures. Therefore, they may boil at the bottom and only steams percolate throughout the fracture, probably resulting in the fracture closure only at the bottom. In cases of semi-isenthalpic ascending with less enthalpy losses, the fluids may also boil at the bottom. Although the fluids may dew at certain depths depending on their degrees of enthalpy loss, the dewed fluids may not precipitate quartz sufficiently for the fracture closure.

On the other hand, the fluids may boil at around the top (probably at several hundred meters below the surface) if the enthalpy losses are adequate. In this case, the largest amount of precipitation may occur at around the top during an early stage. However, an increase in the fluid pressure due to the fracture closure results in a shift of the boiling depth upward. Also, the increase in the fluid pressure decreases the pressure gradient at around the top, resulting in a deceleration of the precipitation. Hence, the amount of the following precipitation at the bottom may exceed those at around the top after a certain duration.

It is quite interesting that the fluids may boil at the bottom or otherwise at around the top depending on their degrees of enthalpy loss. No condition for the fluids to boil at intermediate depths could be found in the present analyses. Those results imply that there may be threshold values of the degrees.

The fluids may not boil when the amounts of enthalpy loss are large, probably resulting in the same properties as the slowly ascending fluids.

The analytical results of the both simplified fluid ascending processes (a) and (b) indicate that the fractures may close mostly at their bottoms.

It should be noted that the above conclusion may be applicable for the fluid ascending systems from any depth. That is, there may be no inevitability for the fracture closure at around the depths of earthquakes.

Keywords: fluid, fracture, quartz, fault, fluid pressure, fault-valve

SCG060-10

Room:302

Time:May 25 11:00-11:15

Effects of Al on kinetics of precipitation of silica minerals from aqueous fluids under crustal conditions

Hanae Saishu^{1*}, Atsushi Okamoto¹, Noriyoshi Tsuchiya¹

¹Tohoku university

Silica is a dominant component in the Earth's crust. Because of high solubility of silica in aqueous fluids and its dependency on P-T conditions, dissolution and precipitation processes of silica minerals play significant roles on the spatial and temporal distributions of fluids and rock strength in the crusts. An ubiquitous occurrence of quartz veins in the vicinity of seismogenic zones implies the importance of the sealing of fractures by quartz on the earthquake cycle.

In spite of the importance of the kinetics of silica precipitation, the complete expression of the rate equation has not been determined, except for precipitation rates on surface reactions (Rimstidt & Barnes, 1980). The difficulty in the estimates of the precipitation rate is arisen from the following reasons. First, although quartz is the most stable silica minerals in the crust, cristobalite and amorphous silica occur in the geothermal areas (Alekseyev et al., 2009). Second, precipitation of silica minerals occurs not only on quartz surfaces but also via nucleation processes in fluids. Third, trace elements including Al³⁺, Na⁺ and K⁺ in solutions affect on the species and kinetics during silica precipitation (Okamoto et al., 2010). Feldspars are dominant constituents of the crust, and thus the effects of these minor components are crucial for considering the silica precipitation in the crust.

In this study, we conducted the hydrothermal flow-through experiments to investigate the overall precipitation rate of silica minerals and the effects of Al in the solutions under crustal conditions (430 C and 31 MPa). The experimental apparatus is similar to that in Okamoto et al. (2010). For precipitation of silica minerals, we used a blank vessel that does not include any rock/mineral substrates. The Si-supersaturated solutions (300-350 ppm, C/C_{eq} = 3-3.5) were prepared by dissolution of quartz at 350 °C, and the concentration of Al in the input solution was controlled by dissolution of albite or granite with different temperatures. The Al and Na (and K in the case of granite) included in the input solutions from 0 to 7 ppm, and the atomic ratio of Al and Na were unity, that is same as the stoichiometry of albite.

The experiments in pure Si solution revealed that the precipitation via nucleation in fluids was approximated as the first-order reaction that is the same as the precipitation on the pre-existing quartz surfaces. Activation energy of precipitation of silica minerals from the solution was estimated to be 39 kJ/mol. In solutions in absence of Al, amorphous silica precipitated. With increasing Al and Na contents in the solutions, the dominant silica mineral systematically changes from amorphous silica, cristobalite to quartz. An important observation is that the logarithmic precipitation rate increased linearly with increasing the Al concentration. Combining these results and the surface reaction rate obtained in the previous study, we obtain the empirical full expression of the rate equation on the silica precipitation that is a function of the degree of supersaturation, temperature, pre-existing quartz surface area, water volume, and Al concentration. One of the implications of this rate equation is that dominant precipitation mechanism changes from surface growth on quartz to precipitation via nucleation, with increasing fracture aperture or decreasing quartz mode in the wall rock in the crust. This is consistent with the observations of natural quartz veins. We will discuss the spatial distribution of silica precipitation and its relationship to the fluid flow in the crusts.

References: Rimstidt, J. D. and Barnes, H. D., 1980, *Geochim. Cosmochim. Acta.*, 44, 1683-1699.; Alekseyev, V. A., Medvedeva, L. S. and Starshinova, N. P., 2009, *Geochem. Int.*, 47, 731-735.; Okamoto A., Saishu H., Hirano N. and Tsuchiya N., 2010, *Geochim. Cosmochim. Acta.*, 74, 3692-3706.

Keywords: silica minerals, aluminum, kinetics, precipitation, hydrothermal experiments, vein

SCG060-11

Room:302

Time:May 25 11:15-11:30

Two primary basalt magmas from NW Rota-1 volcano, Mariana arc, and its heterogeneous mantle diapir

Yoshihiko Tamura^{1*}

¹IFREE, JAMSTEC

Primitive basalts are rarely found in arcs. The active NW Rota-1 volcano in the Mariana arc has erupted near-primitive lavas, which we have sampled with ROV Hyperdolphin (HPD). Samples from the summit (HPD480) and eastern flank (HPD488) include 17 magnesian basalts (51-52 wt % SiO₂) having 7.5-9.5 wt % MgO and Mg# of 61-67, indicating little fractionation. Olivine phenocrysts are as magnesian as Fo₉₃ which contain 0.4 wt % NiO; Cr/(Cr+Al) of spinels are mostly 0.5-0.8, indicating equilibrium with depleted mantle. There are three petrographic groups, based on phenocryst populations: 1) cpx-olivine basalt (COB); 2) plagioclase-olivine basalt (POB); and 3) porphyritic basalt. Geochemical characteristics suggest that POBs formed from lower degrees of mantle melting, or that the COB mantle source was more depleted. On the other hand, they also suggest that COB has a greater subduction component than POB. The calculated primary basaltic magmas of NW Rota-1 volcano (primary POB and COB magmas) indicate segregation pressures of 1.5- 2 GPa (50-65 km deep). These magmas were formed by 15-25 % melting of mantle peridotite having Mg# ~89.5. These two basalt magmatypes are similar to those found for Sumisu and Torishima volcanoes in the Izu-Bonin arc, with COB representing wetter and POB representing drier magmas, where subduction zone-derived melt components are coupled with the water contents. Hydration and partial melting along subducting slabs can trigger Rayleigh-Taylor-like instabilities. Deep subduction components, derived from melting of subducting sediments, play an important role in the generation of NW Rota-1 magmas. Thus, the sediment melting in the underlying slab could have triggered partial melting of hydrous mantle and mantle diapir formation. Moreover, sediment melts may have mixed heterogeneously with hydrous peridotite, which resulted in a mantle diapir consisting of two parts, one poor and another rich in sediment melt.

Keywords: primary magmas, mantle wedge, basalt, arc magmas

Japan Geoscience Union Meeting 2011

(May 22-27 2011 at Makuhari, Chiba, Japan)

©2011. Japan Geoscience Union. All Rights Reserved.



SCG060-12

Room:302

Time:May 25 11:30-11:45

Petrological characteristics of the Finero Phlogopite-Peridotite Massif, Italy

Takahito Suzuki¹, Tomoaki Morishita^{1*}, Akihiro Tamura¹, Masako Yoshikawa², Alberto Zanetti³, Maurizio Mazzucchelli⁴

¹Kanazawa University, ²Kyoto University, ³CNR-Pavia, ⁴Universita di Modena

At subduction zone, hydrous silica-rich fluids/melts derived from subducting lithosphere are expected to be interacting extensively with the overlying mantle, resulting in arc magmatism and/or enrichment of fluid mobile elements (LILE) in the mantle as a source for the following arc magmatism. Details of metasomatic processes in the mantle wedge are crucial to understand the development of subduction zone through the time, and are, however, still not understood yet. The Finero Phlogopite-Peridotite Massif in the Western Italian Alps is well known as a highly metasomatized peridotite massif, which is characterized by abundant metasomatic minerals, such as phlogopite, amphibole and apatite (e.g., Zanetti et al., *Contrib. Mineral. Petrol.*, 134, 107-122; Morishita et al., 2008 *Chem. Geol.* 25, 99-111). Petrological characteristics of the Finero massif have never been well described yet. We present our recent progresses based on field works, especially focusing on metasomatic silica enrichment, the presence of diverse metasomatic agents, antigorite-talc formation and puseodotachylyte-like rocks.

Keywords: fluid, peridotite, metasomatism, Finero massif

SCG060-13

Room:302

Time:May 25 11:45-12:00

Pressure and temperature dependence of ^{13}C diamond Raman shift determined in-situ to 1.27 GPa and 800 degree C

Shigeru Yamashita^{1*}, Bjorn Mysen²

¹ISEI, Okayama University, ²Geophysical Laboratory, CIW

The pressure- and temperature-dependent Raman shift of synthetic ^{13}C diamond was determined in-situ at temperatures to 800 degree C and at pressures to 1.27 GPa. In-situ experiments were conducted using an Ir-gasketed, externally-heated diamond anvil cell (HDAC) fitted to confocal micro-Raman spectrometer. The pressure dependence of the Raman shift was calibrated to the equation-of-state of pure H_2O (IAPWS-95, Wagner and Pruss, J. Phys. Chem. 31, 2002) with a piece of the ^{13}C diamond aggregate (99% pure) and distilled H_2O loaded in the sample chamber of the HDAC. Temperature was controlled to plus-minus 1 degree C with chromel-alumel thermocouples in contact with the anvils near the sample chamber. To ensure the highest precision of the ^{13}C diamond Raman shift, the emission of the 585 nm Ne line was recorded simultaneously as reference. The in-situ experiments were repeated along four different isochores to cover a wide coverage of pressures at high temperatures (0.38 to 1.27 GPa at 800 degree C). No carbon-bearing species were detected in the H_2O fluids, which means that the ^{13}C diamond does not react with H_2O and the diamond anvils as well during these high temperature and pressure measurements.

Multiple regression analysis demonstrated that the pressure and temperature dependence of the ^{13}C diamond Raman shift can be described by a simple quadratic linear form: $\nu(P, T) - \nu(0.1, 25) = -1.065 (\text{plus-minus } 0.044) \times 10^{-2} T - 1.769 (\text{plus-minus } 0.046) \times 10^{-5} T^2 + 2.707 (\text{plus-minus } 0.249) \times 10^{-3} P$, where $\nu(0.1, 25)$ is the Raman shift at ambient condition (1287 cm^{-1}), T is temperature in degree C and P is pressure in MPa. The average error in the pressure determination with this form is estimated to be plus-minus 0.11 GPa. The pressure derivative and the temperature derivative are both consistent with those of Bassett (Mineral Spectroscopy, 1996) and Schiferl et al. (J. Appl. Phys. 82, 1997), within the uncertainties in the regression analysis. In those previous studies, the pressure dependence was measured at ambient temperature, and the temperature dependence was separately measured at ambient pressure. The present result indicates that the pressure and temperature cross derivatives might be present but are negligibly small over the pressure and temperature conditions investigated.

Keywords: diamond, H_2O fluid, Raman shift, in-situ observation

SCG060-14

Room:302

Time:May 25 12:00-12:15

Chemical compositions of hydrothermal fluids derive from a shallow emplacement granite body in Tsushima, Japan.

Masanori Kurosawa^{1*}, Ki-Cheol Shin², satoshi ishii³, Kimikazu Sasa⁴

¹Life Env. Sci., Univ. Tsukuba, ²Res. Inst. Hum. Nat., ³Res. Fac. Center, Univ. Tsukuba, ⁴Puru Appl. Sci., Univ. Tsukuba

Fluid inclusions in quartz from miarolitic cavities, quartz veins, and a Pb-Zn ore deposit at the Miocene granite pluton, Tsushima Islands, Japan, were analyzed by particle-induced X-ray emission (PIXE) to examine chemistries and behaviors of hydrothermal fluids in granite body with shallow emplacement level. The Tsushima granite pluton is mainly composed of biotite-granites and numerous mafic microgranular enclaves. Small miarolitic cavities are relatively common in the granite, and quartz veins are rare. An estimated emplacement level of the granite is 2-6 km deep. Quartz in the miarolitic cavities and the quartz veins contains abundant polyphase inclusions with large halite crystal and vapor-rich inclusion, a small amount of liquid-rich two-phase inclusion, and a few low-salinity liquid-rich inclusion and CO₂ inclusion. Salinities of the polyphase inclusions were of 28-60 wt % NaCl eq., and the homogenizing temperatures (Th) ranged from 460 to 200 C. Two-phase inclusions of the miarolitic cavities showed almost Th of 400-200 C. Quartz in the ore vein contains abundant two-phase inclusion, and a few polyphase inclusion, vapor-rich inclusion, low-salinity liquid inclusion, and CO₂ inclusion. Salinities of the polyphase inclusions were of 28-49 wt % NaCl eq., and the Th ranged from 450 to 250 C.

Element concentrations (average) of polyphase inclusions in the miarolitic cavities, determined by PIXE, were as follows: about 25 wt.% for Cl, 1-5 wt.% for Fe and K, several hundreds to several thousands ppm for Ca, Mn, Ba, Zn, Pb, Br, 200-400 ppm for Cu and Rb, and several tens ppm for Sr and Ge. The compositions are thought to correspond to the original contents of hydrothermal fluid released from the Tsushima granite during solidification. The determined values are several times higher than the values of original hydrothermal fluid estimated from miarolitic quartz from the Miocene Kofu granite (Japan) that has relatively deeper emplacement level (5-8 km deep). The polyphase inclusions of the Tsushima granite were probably formed by decompression boiling of the original hydrothermal fluids during the granite solidification because of the shallow emplacement level. The high contents of transition-metal elements in the polyphase inclusions are also attributable to the element partitioning at the phase separation by boiling. Polyphase inclusions in the quartz veins and the ore vein have compositions similar to those in the miarolitic cavities. Br/Cl ratios (by weight) in the liquid-rich two-phase inclusions are mostly less than 0.0034 of sea values: 0.0014 for the miarolitic cavities, 0.0022 for the quartz veins, and 0.0027 for the ore vein, respectively. On the other hand, the polyphase inclusions have higher values of Br/Cl ratios, and the values are different for each occurrence: 0.0015 to 0.0043 for the miarolitic cavities, 0.0020 to 0.0108 for the quartz veins, and 0.0019 to 0.0124 for the ore vein, respectively.

Keywords: Fluid inclusion, trace element, X-ray analysis, granite, PIXE, ion beam

SCG060-15

Room:302

Time:May 25 12:15-12:30

Progress of hydration in olivine-H₂O and orthopyroxene-H₂O systems at Psat

Yuichi Ogasawara^{1*}, Atsushi Okamoto¹, Noriyoshi Tsuchiya¹

¹Tohoku Univ., Japan

Hydration of ultramafic rocks (serpentinization) commonly occurs in mid-ocean ridges, and the extent and distribution of hydrated mantle plays an important role on the global circulation of H₂O fluids. Although there have been several experimental studies on serpentinization (e.g., Martin and Fyfe, 1970; Seyfried et al., 2003), these studies focused only on the H₂O content in the products or solution chemistries. Therefore, fundamental kinetics and mechanism of serpentinization is still poorly understood. In this study, we conducted hydrothermal experiments on serpentinization to clarify the relationship between the temporal evolution of solution chemistry, progress of hydration reaction and textural developments.

The starting materials were powders of olivine (Fo₉₀, Fa₁₀) or orthopyroxene (En₆₅, Fs₃₅) with size of <0.125mm. The powders and the distilled water were set in the batch type vessel (8.8 cm³) made of the stainless steel with water/rock ratio of 1.0. The temperatures were 250 degreeC at the liq-vap saturation curve. The duration was up to 1008 hours. After the experiments, the solid samples were dried at 90 degreeC for one day, and then were analyzed by X-ray diffractometry and Thermogravimetry. The morphology and cross sections of the products were observed by Scanning electron microscope. The solutions were analyzed by ICP-Mass Spectrometry. The pH values of the solution after the experiments were 7.6-8.5 at room temperature. In both systems, hydration reactions proceeded, but show quite different features in the products and solutions. In the Opx-H₂O experiments, chlorite formed on the surfaces of opx grains. The Si concentration increased with time toward 193.8 ppm, whereas the concentration of Mg was 3.42 ppm. The total H₂O content was less than <0.7 wt.% even at 1008 h. The formation of chlorite is different from the common occurrence of talc after orthopyroxene in natural peridotites. The reason is not clear, but one possibility is that higher Fe content in opx used in this study than that in the oceanic peridotites (En > 80). In the Ol-H₂O experiments, the products were composed of serpentine, magnetite with or without brucite. The H₂O content of the samples increased with time, and reached 3.9 wt.% in 1008h. According to the solution chemistry, the progress of serpentinization is divided into three stages. The concentrations of Si and Mg in solutions increased toward 3.66 and 20.54 ppm, respectively (stage 1), and then decreased drastically toward 0.29 ppm and 0.28 ppm at 504 hours, respectively (stage 2). After 504 h, the solution chemistry was nearly stable (stage 3). Accompanying with the change in the solution chemistry, the products varied as follows: After 336 hours (stage 2 and 3), brucite started to form at the contact with olivine within serpentine rims. Also, only lizardite occurs at stage 1 and 2, whereas chrysotile formed with lizardite. According to activity diagram in Mg-Si-O-H system, the solutions at stage 1 and 2 corresponds to the stability field of serpentine, and a drop in Si concentration indicates the shift from the serpentine stability field to serpentine+brucite stability field, that is consistent with the change of the products. These results suggest that serpentinization after olivine is not always simple as $Ol+H_2O=Serp+Br$, but the reactions evolve with time. In common peridotites, Ol and Opx coexisted, and hydrothermal alteration occurs heterogeneously. Our experimental results indicate that olivine-H₂O and opx-H₂O system show a quite different fluid compositions (Si and Mg) and different rate of hydration. We will conduct further experiments with Ol+Opx+H₂O systems, and discuss how hydration proceed in the oceanic seafloors.

References Janecky, D. R and Seyfried, W. E., (1986). *Geochim Cosmochim. Acta* 50,1357-1378 Martin, B and Fyfe, W. S., (1970). *Chem Geol* 6, 185-202 Allen, D. E and Seyfried, W. E, Jr., (2002). *Geochim Cosmochim. Acta* 67, 1531-1542

Keywords: ultrabasic rock, serpentine, subduction zone

SCG060-16

Room:302

Time:May 25 12:30-12:45

Dehydration kinetics of Antigorite by in situ high-temperature IR microspectroscopy

Michiyo Sawai^{1*}, Arisa Hamada¹, Ikuo Katayama¹, Satoru Nakashima²

¹Hiroshima University, ²Osaka University

Previous studies suggested that the dehydration processes of hydrous minerals such as serpentinite play a key role in a generating mechanism of earthquakes in the subducting slabs. These studies indicate that the reaction of released water from serpentinite with subducting slab is thought to be the cause of intra-slab earthquakes. The volume change caused by reaction and the rate of the reaction products are likely to associate with the earthquake generation mechanism. However, the dehydration process and kinetics of serpentinite are still controversial, thus we here in report the dehydration kinetics of serpentinite.

In previous works, the dehydration kinetics of serpentinite was mainly studied by X-ray diffraction analysis which mainly focused on a change of crystal structure and not for states of water (ex. Inoue et al., 2009). Tokiwai and Nakashima (2010) studied the dehydration kinetics of muscovite by using in situ high-temperature IR microspectroscopy which enables to distinguish the water species. Therefore, we investigated the state of the water in serpentinite and determine the dehydration kinetics by using in situ high-temperature IR microspectroscopy.

Serpentinite samples which consist of antigorite were collected from Nomo peninsula in Nagasaki prefecture. Dehydration experiments of antigorite were conducted by using a fourier transform infrared (FT-IR) microscope in Osaka University, temperature set at 650-750 degrees C and atmospheric pressure under Ar stream which flow rate is 60ml/min.

In the case of antigorite of this study, the spectrum at room temperature shows a relatively sharp band at around 3450-3510 cm^{-1} (peak1), around 3570-3595 cm^{-1} (peak2) and around 3655-3660 cm^{-1} (peak3). Serna et al. (1979) reported that peak1 and peak2 correspond to OH with substitution of Al for Si, and peak3 corresponds to Mg-OH bond, respectively. To describe quantitatively the OH decrease, we measured integral intensity (absorbance) from 3200 to 3900 cm^{-1} . And we also applied a Gaussian function to the absorption band in order to split into the three OH elements and analyze each peak with diffusion equation.

Experimental results show that each peak has different dehydration kinetics and activation energy. The diffusion coefficient approximated by diffusion equation indicates that the peak3 is higher than peak1 and 2. And the activation energy calculated from the temperature show that the peak3 is lower than that of peak1 and peak2. These results suggested that OH associated with Mg tends to dehydrate easily than that associated with Al. In addition we have conducted the heating and cooling experiments of antigorite by the same in situ high-temperature IR microspectroscopy. The results show that the dehydration of Mg-OH (peak3) caused earlier than OH related to Al (peak1 and 2) by about 50 degrees C. These results agree with the data of Bromiley and Pawley (2003) which reports that the presence of even small amount of Al can stabilize antigorite to about some degrees higher temperature.

Keywords: serpentine, dehydration kinetics, diffusion, in situ IR microspectroscopy

SCG060-17

Room:302

Time:May 25 14:15-14:30

Thermal plume in porous media as revealed by streaming potential

Raphael Antoine^{1*}, Kei Kurita¹, Hiroaki Matsuoka¹

¹Earthquake Research Inst., The University

Fluid flow through porous media is a fundamental process to control fluid flow through the crust and the mantle. It has been extensively investigated for long time both in experimental and theoretical approaches but because of experimental limitations fluid dynamical approach has not been conducted enough in laboratory experiments. The main limitation comes from non-transparency of experimental cell, which is composed of solid framework and fluid in the pore space. Non-transparency of solid medium as well as density mismatch make optical investigation through the working cell difficult. Recently nondestructive tomographic methods such as NMR imaging are applied to derive flow field but it requires large experimental facility and lots of cost. In this presentation we report a trial in combining streaming potential and temperatures to estimate flow field in porous media.

Streaming potential, sometimes called as flow potential occurs when fluid flows through porous/granular material which has ion exchanges with flowing fluid. In the experimental cell of the size of 8x8x20 cm glass beads of homogeneous grain size (0.35 to 4 mm in diameter) are packed and NaCl aqueous solution is used as a working fluid. At the base of the cell we put a small heater (5x3x1 mm) as a localized heat source. Pt electrodes are inserted at several vertical positions above the heater along the center line to measure the induced potential by heating. Temperatures are measured by thermocouples along horizontal line 1cm above the heater and along the vertical centerline.

We measured temporal variations of potential and temperature upon heating with constant power supply to the heater. Systematic variations in the potential were obtained: after small decrease at the initiation large positive increase was observed (the potential signal is measured from the lowest electrode closed to the heater). The amplitude of the initial decrease seems not to depend on the applied power while the succeeding large increase is linearly proportional to the power.

We made numerical simulations to compare both potential and temperature in the corresponding geometry and similar situations as the experiment. We obtained similar behavior which can be interpreted as thermal plume rising above the heater in porous media. Different from laminar thermal plume formulated by Batchelor rising velocity of plume seems to depend linearly on the applied power. This confirms average field formulation of Darcy flow is effective in this permeability range.

Keywords: thermal plume, permeable flow, porous media, streaming potential

SCG060-18

Room:302

Time:May 25 14:30-14:45

Structure around Philippine Sea slab beneath Kii Peninsula inferred from receiver function analysis

Takuo Shibutani^{1*}, Taishi Fukui², Yoichiro Nakagawa³, Kazuro Hirahara², Setsuro Nakao¹, Kazuhiro Nishimura¹, Masayo Sawada¹

¹DPRI, Kyoto Univ, ²Science, Kyoto Univ, ³Hitachi Ltd

1. Introduction

Deep low frequency events (DLFEs) are distributed widely from western Shikoku to central Tokai (Obara, 2002). Results from seismic tomographies and receiver function analyses revealed that the oceanic crust of the Philippine Sea plate has a low velocity and a high V_P/V_S ratio (Hirose et al., 2007; Ueno et al., 2008). Hot springs with high $^3\text{He}/^4\text{He}$ ratios are found in an area between central Kinki and Kii Peninsula despite in the forearc region (Sano and Wakita, 1985). These phenomena suggest the process that H_2O subducting with the oceanic crust dehydrates at the depths of 30 - 40 km, causes the DLFEs, and uprises to shallower depths.

We carried out seismic observations in Kii Peninsula since 2004 in order to estimate the structure of the Philippine Sea plate and the surrounding area. We deploy seismometers in linear order with the average spacing of ~ 5 km and record waveforms of teleseismic events. We applied receiver function analyses shown below to the waveform data, and obtained images of S wave velocity discontinuities. In the previous presentation (Shibutani et al., 2009), we reported the results for three profile lines in the NNW-SSE direction along which the Philippine Sea plate is subducting. In this presentation we will report the results for two new profile lines, one in the NNW-SSE direction and the other in the ENE-WSW direction. We will also discuss the structure around Philippine Sea plate subducting beneath Kii Peninsula based on the receiver function images.

2. Receiver function analysis

Receiver functions are calculated by deconvolving the vertical component from the horizontal component of teleseismic P codas. They consist of PS converted waves generated at S wave velocity discontinuities beneath stations. The relative travel times between the PS converted waves and the direct P wave depend on the depths of the discontinuities and the P and S wave velocities above them, and the relative amplitudes depend on the S wave velocity jump at the discontinuities. In this study we converted the time axis of the receiver functions to the depth axis with the velocity model JMA2001 (Ueno et al., 2002), stacked the amplitudes of the receiver functions on the common conversion points, and obtained images of S wave velocity discontinuities.

3. Structure around Philippine Sea slab

A pair of blue and red lines dipping to northwest can be found as a common feature among the four profiles in the subduction direction. These can be interpreted as the upper surface of the Philippine Sea slab and the oceanic Moho, respectively. The oceanic crust sandwiched in between them shows remarkable low velocity (darker blue) up to the depths of 30 - 40 km where the DLFEs occur. The degree of the low velocity in the oceanic crust decreases beyond the depths.

We can find that another blue line branches off near the DLFE area and extends in the mantle wedge in the receiver function images for three profiles in central to western part of the peninsula. This indicates that the mantle wedge is widely low velocity. The red line showing the oceanic Moho becomes unclear beneath 40 km depth, which suggests that the velocity gap between the oceanic crust and the oceanic mantle becomes small. The configuration of the slab seems to be convex upward.

On the other hand, for the profile in the eastern part of the peninsula, we cannot see that low velocity in the oceanic crust extends to the mantle wedge. The oceanic Moho is uniformly clear from 30 km depth at the southeastern edge to 70 km depth at the northwestern edge. The geometry of the slab is linear.

The differences in the structure and geometry of the slab and the mantle wedge between the central to western part and the eastern part of the peninsula can be explained by the amount of H_2O in the oceanic crust beneath 40 km depth after the dehydration.

Keywords: Philippine Sea slab, Mantle wedge, Slab-derived fluid, Receiver function image, Linear array seismic observation, Kii Peninsula

SCG060-19

Room:302

Time:May 25 14:45-15:00

Li isotope map of geofluid in SW Japan: Is deep-crustal fluid in fore-arc region derived from slab?

Yoshiro Nishio^{1*}, Kohei Kazahaya², Yoichi Oyama²

¹Kochi Institute, JAMSTEC, ²Geological Survey of Japan, AIST

It has been proposed that the island arc deep-crustal fluid has played important role in volcanic and seismic activities, although many things, including the relationships between the island arc deep-crustal fluid and slab-derived fluid, have been still unresolved. It has been difficult to identify the nature of deep-crustal fluid based on the geochemical researches using underground water recovered from spring and well, because the deep-crustal fluid is very diluted by surface water during ascending. Lithium (Li), the lightest alkali metal, is a fluid-mobile element having two stable isotopes, ⁷Li/⁶Li, with abundances of 92.5% and 7.5%, respectively. Amount of Li leached from rock to fluid drastically increases with the temperature, and once leached Li is kept in fluid while decreasing temperature (cooling). These features indicate that non-traditional Li isotopic tracer has a great potential to provide new insight on the origin of nature of island arc deep-crustal fluid.

It has been expected that Li isotopic compositions of underground water samples whose Li/Cl ratios are significantly high were not affected by surface water (Nishio et al., 2010). Therefore, to reveal Li isotopic distribution of deep-crustal fluids, we have analyzed Li isotopic compositions of underground water samples whose Li/Cl ratios are significantly high. In this study, the analyzed samples have been recovered from SW Japan (excluding Kyushu area).

The results show that ⁷Li/⁶Li of near-trench samples are significantly higher than those of other samples. This result means that Li in deep-crustal fluids beneath forearc region in SW Japan are derived from subducted Philippine Sea slab. The results, furthermore, reveal that relatively ⁷Li/⁶Li ratios are observed in underground water samples from the western Kii Peninsula where is located in forearc region. Thus, Li isotopic results have presented us new knowledge for island-arc deep-crustal fluid.

Acknowledgements:

We thank for M. Yasuhara, T. Satoh, N. Morikawa, H. Takahashi, A. Inamura, H. Tsukamoto, A. Shibahara, K. Tanaka for sampling assistance.

Reference:

Nishio et al., 2010, EPSL 297, 567-576.

Keywords: geofluid, deep-crustal fluid, lithium isotope, SW Japan, slab-derived fluid, Philippine Sea plate

Japan Geoscience Union Meeting 2011

(May 22-27 2011 at Makuhari, Chiba, Japan)

©2011. Japan Geoscience Union. All Rights Reserved.



SCG060-20

Room:302

Time:May 25 15:00-15:15

Characteristics of shallow low-frequency events suggested from numerical simulations

Keisuke Ariyoshi^{1*}, Toru Matsuzawa², Takane Hori¹, Ryoko Nakata¹, Jean-Paul Ampuero³, Ryota Hino², Akira Hasegawa², Yoshiyuki Kaneda¹

¹DONET, JAMSTEC, ²RCPEV, Tohoku University, ³California Institute of Technology

Recently, non-volcanic low-frequency events have been observed along plate boundaries in subduction zones of the world. It is well-known that the low-frequency events occur in the transition zones between the seismogenic zones and the stable-sliding zones, and migrate along strike direction of subduction plate boundaries. On the basis of these characteristics, some numerical simulation studies have tried to estimate the possible ranges of parameters such as frictional stability and pore-pressure, which enables us to know the preseismic change in the activity of the low-frequency events. However, characteristics of the low-frequency events occurring in the shallower part have not been clear. In this study, we perform a numerical simulation with numerous small asperities which generate low-frequency events in the shallower part of a subduction plate boundary, and try to investigate their preseismic change.

Keywords: slow earthquake, migration process, stress perturbation due to great asperity, subduction zone, rate- state dependent friction law, numerical simulation

SCG060-21

Room:302

Time:May 25 15:15-15:30

Spatial distribution of high- and low-frequency earthquakes among the aftershocks of the Iwate-Miyagi Nairiku Earthquake

Masahiro Kosuga^{1*}, The group for the aftershock observations of the Iwate-Miyagi Nairiku Earthquake²

¹Graduate School of Science & Technology, ²GIMNE2008

1. Introduction

Low-frequency earthquakes (LFEQs) have been attracted the interest of seismologists by their waveform characteristics that reflect the unusual source processes. Some LFEQs occur as the aftershocks of large earthquakes. Here we detect LFEQs from the aftershocks of the Iwate-Miyagi Nairiku Earthquake in 2008 and investigate their spatial distribution to get insight to their origin.

2. Data and method

We detect LFEQs by using the predominant frequency of Fourier spectral amplitude for both body wave and coda wave observed at 59 temporal stations operated by the group for the aftershock observations. The predominant frequency depends both hypocentral distance and earthquake magnitude. Thus we first estimate the zero-offset frequency for each earthquake by straight line fitting between the logarithm of predominant frequency and the hypocentral distance. Then we performed a linear regression between the logarithm of zero-offset frequencies and the earthquake magnitudes. We define the frequency deviation for each earthquake by the frequency difference from the regression line. On the scatter plot between the frequency deviation for body wave as the horizontal axis and those for coda wave as the vertical axis, there is a clear positive correlation. We define high-frequency earthquakes (HFEQs) and LFEQs as those in the first quadrant and third quadrant on the scatter plot, respectively, with larger frequency deviation than the standard deviation.

3. Spatial distribution of high- and low-frequency earthquakes

HFEQs are distributed preferentially in the source area of main shock, in particular, in a wide area to the north of mainshock and a linear zone to the SSE of mainshock. On the other hand the LFEQs are distributed complementarily to the HFEQs, in a wide area to the WNW and to the SWS of mainshock, and outside the source area both to the north and to the south. Compared with the geology, the LFEQs are located around the Kurikoma and Yakeishi volcanoes, and in the calderas formed from the Pliocene to the early Pleistocene in age. This suggests that these LFEQs occur in hotter areas where the ductile deformation occurs. Not a few LFEQs occur in a northern extension of seismogenic fault, where postseismic deformation was observed by GPS. This deformation is attributed to the aseismic slip on a fault that did not move coseismically. The LFEQs in the area are located along a deep boundary of aseismic fault. The HFEQs occur on the seismogenic fault that is located to a deeper extension of aseismic fault. This spatial pattern suggests the effect of both the increased pore pressure and the decreased normal stress on the faults as the location moves from the deeper part to the shallower part. Thus the distribution of LFEQs is a key parameter to interpret the role of crustal fluids to the seismogenic processes.

Keywords: low-frequency earthquakes, aftershocks, Iwate-Miyagi Nairiku Earthquake, geofluid

Japan Geoscience Union Meeting 2011

(May 22-27 2011 at Makuhari, Chiba, Japan)

©2011. Japan Geoscience Union. All Rights Reserved.



SCG060-22

Room:302

Time:May 25 15:30-15:45

Electromagnetic measurements to image geofluid in three-dimensions under NE-Japan arc

Yasuo Ogawa^{1*}, Masahiro Ichiki², Takao Koyama³, Hiroaki TOH⁴, Masaki Matsushima⁵, Wataru Kanda¹, Hiromi Fukino⁵, Yoshimori Honkura⁵, Makoto Uyeshima³

¹VFRC, Tokyo Inst. tech, ²Tohoku University, ³University of Tokyo, ⁴Kyoto University, ⁵Tokyo Institute of Technology

Fluids in the crust play an important role in volcanic processes and earthquake generation processes. Electrical resistivity is a geophysical parameter which is sensitive to the existence and connectivity of fluids. Thus, by imaging the resistivity by electrical induction method such as magnetotellurics, we can get important information on the amount, chemical composition and transport properties of fluids.

We have started magnetotelluric measurements in the NE Japan using wideband (0.01s–1000s) and long period (10s?20,000s) measurements. The wideband measurements are focused around the Onikobe caldera and the surrounding regions. In 2009, Thirty magnetotelluric soundings were carried out in and around the Onikobe caldera. We have found the lower crustal conductor with N-S strike directions and its shallower continuation to the Onikobe caldera, which has E-W directions representing the E-W tectonic compression. In 2010, we had 30 more stations to the south of the Naruko volcano, covering 20km x 20km.

In addition to the wideband measurements, we have made long period measurements to image the upper mantle structure. We have 32 long period stations with 20km grid spacing in order to image the upper mantle.

We will show some preliminary results on those on-going measurements.

Keywords: geofluid, magnetotellurics, electromagnetic method, resistivity

SCG060-23

Room:302

Time:May 25 15:45-16:00

Electrical conductivity of fluid-bearing crustal rock under high pressure

Akira Shimojuku^{1*}, Takashi Yoshino¹, Daisuke Yamazaki¹

¹Okayama University, ISEI

It has been reported that the electrical conductivities determined by magnetotelluric methods in the lower crust are much higher than those determined by dry laboratory samples of crustal rocks. The aqueous fluid is the most likely reason for the high-conductivity anomaly regions (e.g., Shankland and Ander, 1982). Since the solubility of silicate component in the aqueous fluid should increase with increasing pressure (Manning, 1994), the electrical conductivity of fluid-bearing rocks can be higher at pressure of the lower crust. To examine the effect of the soluble ionic species in aqueous fluid on the bulk rock conductivity, we measured the electrical conductivity of fluid-bearing quartzite as functions of temperature and fluid content under high pressure.

High-pressure experiments were carried out using a DIA-type high-pressure apparatus. Pyrophyllite was used as a pressure medium, and cylindrical graphite was used as a furnace. We used two kinds of the starting materials. One is the sintered quartz aggregate, which was synthesized from the mixture of quartz reagent and silicic acid using a piston-cylinder high-pressure apparatus. The other is chert generated from Tanba district, Japan. These starting materials initially contain 200-5560 wt. ppm H₂O as a fluid inclusion and OH species. To prevent a loss of water during the electrical conductivity measurements, we used a diamond single crystal capsule. Electrical conductivity was measured using the impedance spectroscopy method. Experiments were conducted at 1 GPa. Temperature range was from 700 to 1450K. The texture of the recovered samples was observed using field-emission scanning electron microscope, and the fluid content was measured using Fourier transformed infrared spectroscopy and calibration proposed by Paterson (1982).

The electrical conductivity increases proportional to (fluid fraction)^{0.86}. Our result suggests that the observational electrical conductivity at Tohoku, Japan (Ogawa et al. 2001) and New Zealand (Wannamaker et al. 2009) in the middle crust is unable to account for quartz plus H₂O. Therefore, plausible explanations of high-conductivity anomaly are presence of saline fluid and/or the other ionic species.

Keywords: electrical conductivity, fluid, crust

SCG060-24

Room:302

Time:May 25 16:00-16:15

Comprehensive geochemical model for the melting of mantle metasomatized by slab-derived fluid

Hitomi Nakamura^{1*}, Hikaru Iwamori¹

¹Tokyo Institute of Technology

The chemical composition of a relatively undifferentiated volcanic rock in arc has the integrated information of the processes occurred beneath a volcano in the mantle wedge, such as material infiltration from the subducting slab and subsequent melting of the mantle. Here, we aim to reveal how the whole rock composition including isotopic ratios and trace element abundances can be quantitatively explained by a series of the relevant processes in the mantle, based on which we constrain the geochemical cycling and thermal structure in subduction zones.

We apply a mass balance model to the Quaternary volcanic rocks of Central Japan where the two oceanic plates obliquely subducts. The compositions of slab-derived fluids can be estimated starting from subduction and dehydration of oceanic crustal materials. Then the composition of fluid-metasomatized mantle, including the amount of slab-derived fluids, is estimated based on isotopic systematics as in Nakamura et al. (2008). The composition of subsequent product (i.e., primary arc magma) is then predicted from that of the estimated metasomatized mantle as a forward model. Finally, by optimizing two important parameters involved in the melting equation (i.e., degree of melting and garnet/spinel lherzolite ratio involved in the melting), we have been successful to inverse these parameters based on the observed compositions of volcanic rocks.

As a result, the condition of magma genesis beneath the Central Japan arc is characterized by relatively high fluid fractions, low melting degrees of melting and high proportions of garnet lherzolite in the melting source region, compared to those of neighboring arcs with single subducting plates. The low melting degree and high garnet contribution may imply a low geothermal gradient and near-solidus melting over the spinel-garnet transition depths, semi-quantitatively constraining the thermal structure beneath Central Japan. The results are consistent with the independent numerical modeling of the region, suggesting a cold environment due to overlapping subduction of the Pacific and Philippine Sea plates.

In spite of the cold environment, adakitic rocks commonly occur in the investigated region. The mass balance model of this study demonstrates that the high fluid fraction, low melting degree of garnet lherzolite (plus subsequent crystal fractionation that shifts the overall abundances without modifying the characteristic patterns such as Sr/Y ratio) may explain the adakite signature in the cold environment. We suggest that the mass balance model is a promising approach to constrain the fluid and melting processes as well as the mantle thermal structure in subduction zones.

Keywords: slab, slab-derived fluid, geofluid, subduction, magma, volcano

SCG060-P01

Room:Convention Hall

Time:May 25 16:15-18:45

Understanding the dynamics of thermo-chemical mantle wedge based on a simple model

Satoru Honda^{1*}, Taras Gerya², Guizhi Zhu²

¹ERI, Univ. Tokyo, ²ETH Zurich

Complex dynamical phenomena may be expected in the mantle wedge, since it will be controlled by a combination of thermal and chemical effects. Recent our studies show the possibility of the existence of small-scale convection in the mantle wedge, which may be driven by thermal/chemical buoyancies. Such a small-scale convection may explain the along-arc variation of arc volcanism. In order to understand the complex phenomena associated with thermal and chemical effects, we have constructed a simplified model of thermo-chemical convection in the mantle wedge. In this model, we assume the kinematic flow of a chemical agent, such as water, from the top of the subducting slab. This chemical agent affects both the density and the viscosity of the region where it resides and decreases the density and viscosity.

We found that major effects of this low density and viscosity anomaly is to suppress the three-dimensional characteristic of mantle flow. Chemically polluted, thus buoyant region tends to stagnate and this results in the low temperature zone in the corner of mantle wedge. This result suggests the chemical origin of non-moving mantle part in the corner of the mantle wedge (nose), which is sometimes necessary to explain the low heat flow in the fore-arc. We also constructed a hybrid model: The chemical agency close to the trench affects both density and viscosity and it in the back arc region does only the viscosity. The model shows the co-existence of the low temperature nose and the small-scale thermally driven convection in the back arc. This may explain some of the geologic character of the northern Honshu arc.

Keywords: subduction zone, small-scale convection, water, arc volcanism

SCG060-P02

Room:Convention Hall

Time:May 25 16:15-18:45

Depth Dependence of Subduction Zone Seismicity and its Uniformity

Keiko Kuge^{1*}

¹Dept. Geophysics, Kyoto University

Arc volcanoes are typically located where the subducting slab is ~110 km deep (e.g. Tatsumi, 1986). To explain the uniformity of the arc volcano configuration, Wada and Wang (2009) proposed subduction zone thermal models with common decoupling depth, in which the interface between the slab and the mantle wedge is decoupled to a depth of 70-80 km where mantle wedge flows are not dragged by the subducting slab. If the thermal models really dominate, not only thermal structure but also earthquake activity in subduction zones can be affected because the condition of temperature controls seismogenesis at plate boundaries and within slabs. In this study, I attempt to diagnose the models of Wada and Wang (2009) by examining variation of seismic activity with depth in subduction zones.

Using earthquake hypocenter data relocated by the method of Engdahl et al. (1998), I examine dependence of earthquake frequency on depth down to 200 km. In subduction zones with thermal parameters larger than 800 km, the number of earthquakes exponentially decreases with depth below ~50 km, and the decreasing rate changes at depth of 75-100 km. The depth changing the decreasing rate seems to be uniform in the subduction zones, having no significant correlation with the thermal parameters. Depth distribution of earthquakes deeper than 75-100 km tends to depend on subduction zones. In some subduction zones the earthquake frequencies continue to be at low rates, whereas there are dominant peaks of earthquake activity at depths in some subduction zones. The similar observations are also obtained in the Global CMT catalogue.

Using the Global CMT catalog, I examine the depth distribution of earthquakes which depends on focal mechanisms. The depth of 75-100 km is close to the lower limit where thrust earthquakes occur. Low-angle thrust earthquakes, which may be plate-boundary earthquakes, occur at depths shallower than 75 km. My waveform modeling for some low-angle thrust earthquakes shows that the depths are shallower than ~50km. The depth of 75-100 km is a turning depth where focal mechanisms change. Therefore, change in earthquake frequency at depth of 75-100 km can be a manifestation of two features: Vanishing of thrust earthquakes above 75 km and no significant increase of slab earthquakes at depths of 75-100 km shallower. Taking account of the dependence of the two features on temperature, the uniformity observed for the variation of seismic activity with depth in subduction zones is consistent with the thermal models of Wada and Wang (2009).

SCG060-P03

Room: Convention Hall

Time: May 25 16:15-18:45

Major and Trace elements mineral composition in peridotites from the Ust'-Belaya ophiolite, Far East Russia

Sumiaki Machi^{1*}, Akira Ishiwatari², Tomoaki Morishita³, Yasutaka Hayasaka⁴, Galina V. Ledneva⁵, Borys A. Bazylev⁵, Sergei D. Sokolov⁵, Suren A. Palandzhyan⁵, Akihiro Tamura³, Shoji Arai⁶

¹Natural Sci. & Tec., Kanazawa Univ., ²NE Asia Center, Tohoku Univ., ³FSO, Kanazawa Univ., ⁴Earth & Planet. Sys. Sci., Hiroshima Uni., ⁵Geol. Inst. Russia Academy of Science, ⁶Earth Sci. Course, Kanazawa Univ.

The Ust'-Belaya ophiolite is exposed in the 80 km x 40 km area on the south of Ust'-Belaya (N65 30', E173 17'), Far East Russia (Sokolov et al., 2003, Geol. Soc. London, Spec. Publ., 218, 619-). The associated limestone suggests Devonian or older age of this ophiolite. It is an important character of this ophiolite that glaucophane-bearing rocks occur. Here we report the petrographical features and mineral chemistry of the peridotite from the Ust'-Belaya ophiolite and discuss about their metamorphism and metasomatism.

Mantle section of the Ust'-Belaya ophiolite is composed of fertile lherzolite to moderately depleted harzburgite. As a result of significant hydration, those peridotites contain various hydrous minerals such as amphibole, talc, secondary clinopyroxene and antigorite. In some of antigorite-bearing peridotites, olivine shows an apparent "cleavage". Such petrographical characteristics resemble those of the antigorite-bearing serpentinite from Mariana forearc (Ohara & Ishii, 1998, Island Arc, 7, 541-; Murata et al., 2009, Geosphere, 5, 90-).

Cr# of spinel in the Ust'-Belaya peridotite shows wide range from 0.1 to 0.5, which is similar compositional range to these of the mid ocean ridge peridotites. It is noteworthy that low-Cr spinel (Cr#=0.1) coexist with high-Na clinopyroxene. Such Na-cpx shows similar trace element pattern to the mid ocean ridge peridotite, which is explained by simple extraction of melts. Therefore such Na-rich clinopyroxene bearing peridotite may represent the deeper level of melting column. On the other hand, the other clinopyroxenes show LREE-enriched trace elements patterns, which is cannot be explained by simple extraction of melts. These patterns can be explained by influx melting.

Amphiboles show different compositional trend corresponding to the mineral assemblage. In Atg-free type rocks, amphibole covers a compositional range from tremolite to pargasite. Meanwhile, in Atg-bearing type rocks, amphibole covers a compositional range from tremolite to richterite with edenite. Trace elements patterns of the former amphiboles (magnesiohornblende) are similar to those of clinopyroxenes in the same sample. Therefore the fluid related to the influx melting was able to be responsible for the formation of these amphiboles. On the other hand, the latter amphiboles (Na-rich tremolite/richterite) shows low concentration and pronounced positive anomaly for Sr. This indicate introduction of Na and Sr coupled with removal of these elements.

The influx melting inferred from trace elements patterns of cpx, as well as the occur of glaucophane-bearing rocks, low equilibrium temperature of peridotites and the evidence of fluid-peridotite interaction are suggesting the Ust'-Belaya peridotite may represent a fragment of the pre-late Paleozoic forearc mantle wedge. Absence of highly depleted peridotite suggests that highly depleted peridotites are not necessary for every forearc environments.

Keywords: subduction zone, antigorite, amphibole, serpentinization

SCG060-P04

Room:Convention Hall

Time:May 25 16:15-18:45

XANES study on the redox state of silicate glasses in: a preliminary result for boninites from Ogasawara Islands, Japan

Hidemi Ishibashi^{1*}, Shoko Odake¹, Hiroyuki Kagi¹

¹Geochemical Research Center, Univ. Tokyo

The redox state of arc mantle is not only of geochemical interest but also an important factor to understand processes of material cycle and generation of arc magma within mantle wedge. Previous studies on mantle xenoliths indicated that arc mantle is more oxidized relative to those of other tectonic settings and proposed that the oxidized nature is attributed to an influence of subduction-related fluid. However, it is unobvious that partially melted region within mantle wedge where arc magma is generated is actually oxidized because mantle xenoliths are fragments of cool, rigid, re-equilibrated lithospheric mantle. In addition, the role of subduction-related fluid on oxidization of arc mantle is still unclear.

Arc magmas might be a unique material having information about the redox state of their source mantle region. Among various arc magmas, we thought that boninite is most suitable to examine both the redox state of arc mantle and the effect of subduction-related fluid. This is because they are undifferentiated and their modification during ascent was minimal. In addition, they were considered to be generated by partial melting of hydrous mantle which was highly influenced by subduction-related fluid. Therefore, the redox state of boninite is expected to have a key to clarify above issues.

It is well known that valence state of Fe in silicate glass is a sensitive indicator of its oxygen fugacity (fO_2) and can be determined from pre-edge feature in Fe K-edge XANES spectrum. In this study, we investigated fO_2 of silicate glasses included in three boninite pillow lavas from Chichijima and Mukojima, Ogasawara islands, Japan, using Fe K-edge micro X-ray absorption near-edge structure (XANES) spectroscopy. A natural glass included in pahoehoe lava from Kilauea volcano, Hawaii was also analyzed for comparison. We performed the measurements using Beam Line 4A in Photon Factory, KEK, which enables us micro analysis of XANES. The obtained spectra were analyzed using the method of Cottrell et al. (2009). Two pre-edge peaks centered at ca. 7112eV (peak-1) and ca. 7114eV (peak-2), respectively, are commonly observed for silicate glass. The former and the latter are attributed to absorptions by Fe²⁺ and Fe³⁺ in silicate glass, respectively, and intensity ratio of peak-2 to peak-1 increases with increasing Fe³⁺/Fe²⁺ ratio. Therefore, the intensity ratio is a useful indicator of fO_2 for silicate glass. We estimate fO_2 of silicate glass using the relation between the intensity ratio and fO_2 based on experimental dataset for basaltic glass (Cottrell et al. 2009).

We measured several points of groundmass glasses for each lava samples and confirmed that groundmass glass is homogeneous in terms of Fe³⁺/Fe²⁺ ratio for the studied samples. Delta QMF (Quartz-Magnetite-Fayalite) value [= log fO_2 (sample) ? log fO_2 (QMF buffer)] of +0.2 was obtained for Kilauea pahoehoe glass. This is consistent with previous studies, demonstrating reliability of this method. Delta QMF values are +0.7 for a samples from Chichijima and +0.5 and +1.3 for two samples from Mukojima, respectively. With considering the fact that the intensity ratio is higher for silicic glass than for basaltic glass at the same Fe²⁺/Fe³⁺ ratio and boninite is more enriched in SiO₂ than basalt, the boninites may be more reduced than the estimated fO_2 conditions. In addition, previous study showed that crystallization of mafic silicate minerals slightly oxidizes silicate melt and the effect of dehydration during ascent on fO_2 of silicate melt is negligible. This suggests that the redox condition of primially boninite melt, and hence of its source mantle, was at least more reduced than the estimated fO_2 (near QMF buffer) whereas it was highly influenced by subduction-related fluid. Therefore, the effect of subduction-related fluid on the redox state of partially melted arc mantle is considered to be minor.

Keywords: XANES, arc mantle, boninite, redox state, oxygen fugacity, silicate glass

SCG060-P05

Room:Convention Hall

Time:May 25 16:15-18:45

Partial melting in deep subduction zone detected from zircon preserved in the Sanbagawa eclogite

Miyuki Arakawa^{1*}, Kazuaki Okamoto¹, Yukiyasu Tsutsumi², Terabayashi Masaru³

¹Saitama University,Japan, ²National Science Museum, ³Kagawa University,Japan

Subducting oceanic plate is dehydrated due to metamorphic reaction in higher pressure and temperature conditions. The dehydrated fluid is considered to cause deep focused earthquake and Island Arc volcanism. Recently we have discovered an eclogite outcrop exhibiting partial melting texture from the Sanbagawa high P/T metamorphic belt, characterized as subducted oceanic material (Okamoto & Arakawa, 2011). The discovery is significantly important because the melt may play an important role in deep-focused earthquake and the melt itself directly may contribute to the origin of Island Arc magma. Due to an extensive retrograde hydration and deformation, melting process is only preserved in garnet on thin section. Zircon is the best tool to reconstruct melting process at eclogite facies condition because it preserves 1) high P minerals, 2) melt and fluid as inclusion and 3) the zircon growth history can be traced from its zonal texture.

Analytical method

We carefully collected the eclogite (SHT15) and the melted portion (SHT16) characterized as quartz-plagioclase rich domain from the outcrop exhibiting melting texture. Zircon separation was based on Tsutsumi et al. (2009). One another sample (SHT17) showing the eclogite with minor melted texture was also collected. Separated zircons from the above three specimens were carefully observed under SEM, CL, and the zircon inclusions were identified using EDS and laser Raman.

Result

The zircons from the eclogite portion (SHT15) are elongated and have relatively large diameters in 100 to 250 microns. The zircons from the melted portion (SHT16) are rounded and 100 to 200 microns. The specimens SHT17 have elongated and rounded zircons. Zonal textures in the zircon from the SHT15 are classified as core, mantle and rims. Zircons from the melted portion (SHT16) have homogeneous core with thin mantle and rims. Zircon inclusions from the core (SHT15 and SHT17) are characterized as igneous and altered phase (apatite and gypsum). Rutile and amphibole are recognized from the mantle.

Discussion and conclusion

The zircon features from the melted portion (SHT16) are identical with the zircons (GO4) from the quartz bearing eclogite described by Okamoto et al. (2004). The GO4 zircons are considered as grown at prograde stage (120 to 110 Ma). The zircons from the SHT15 and SHT17 are comparable with zircons from the metasedimentary rock (QM) associated with the quartz bearing eclogite (Okamoto et al. 2004). The QM zircons have detrital core with metamorphic mantle grown at 120-110 Ma and thin rims. These lines of evidence suggest that the Sanbagawa eclogite suffered partial melting in deep subduction zone. Under the micron scope, mylonite texture is obvious in thin sections from the specimen SHT16. It may suggest that semi-brittle deformation was caused by partial melting and the melt accumulation was also governed by the deformation.

Keywords: deep subduction zone, partial melting, eclogite, zircon

SCG060-P06

Room:Convention Hall

Time:May 25 16:15-18:45

Velocity and conductivity measurements on synthetic wet halite rocks at high pressure and temperature

Tohru Watanabe^{1*}, Motoki Kitano¹

¹University of Toyama

Intercrystalline fluid can significantly affect rheological and transport properties of rocks. Its influences are strongly dependent on its distribution. The dihedral angle between solid and liquid phases has been widely accepted as a key parameter that controls solid-liquid textures. The liquid phase is not expected to be interconnected if the dihedral angle is larger than 60 degree. However, observations contradictory to dihedral angle values have been reported. Watanabe and Peach (2002) suggested the coexistence of grain boundary brine with a positive dihedral angle. For good understanding of fluid distribution, it is thus critical to study the nature of grain boundary fluid.

We have developed a high pressure and temperature apparatus for study of intercrystalline fluid distribution. It was specially designed for measurements of elastic wave velocities and electrical conductivity. Elastic wave velocities (V_p and V_s) and electrical impedance can be measured to constrain intercrystalline fluid distribution. The apparatus mainly consists of a conventional cold-seal vessel with an external heater. The pressure medium is silicon oil of the viscosity of 10 Pa s. The pressure and temperature can be controlled from 0 to 200 MPa and from 20 to 200 C, respectively. Dimensions of a sample are 9 mm in diameter, and 15 mm in length.

Halite-water system is used as an analog for crustal rocks. The dihedral angle has been studied systematically at various pressure and temperature conditions [Lewis and Holness, 1996]. The dihedral angle is larger than 60 degree at lower pressure and temperature. It decreases to smaller than 60 degree with increasing pressure and temperature. A sample is prepared by cold-pressing and annealing of wet NaCl powder. Optical examination has shown that synthesized samples are microstructurally homogeneous. Grains are polygonal and equidimensional with a mean diameter of 300 micrometer. Grain boundaries vary from straight to bowed and 120 degree triple junctions are common. Gas and fluid bearing inclusions are visible on the grain boundaries. There are spherical inclusions or isolated worm-like channels.

In this poster, we will report preliminary results of compressional wave velocity and electrical conductivity measurements.

Keywords: elastic wave velocity, electrical conductivity, halite, water

SCG060-P07

Room:Convention Hall

Time:May 25 16:15-18:45

CO₂ bearing saline aqueous fluid inclusions in olivine of peridotite xenoliths of Pinatubo 1991 ejecta

yoshitaka kumagai^{1*}, Tatsuhiko Kawamoto¹, Masako Yoshikawa¹, Tetsuo Kobayashi²

¹Inst. Geothermal Sci., Kyoto Univ., ²Earth and Environ. Sci., Kagoshima Univ.

Spinel peridotite xenoliths are present in the dacitic rocks of the Pinatubo 1991 eruption, Luzon Island, Philippines. The Pinatubo volcano is one of the Bataan arc-front volcanoes that are associated with eastward subduction of the South China Sea floor along the Manila Trench. Peridotite xenoliths are mainly composed of olivine and orthopyroxene, with minor amounts of spinel and calcic amphibole surrounding spinel and orthopyroxene. Small grains of clinopyroxene and phlogopite also surround spinel and orthopyroxene. Phlogopite and amphibole inside of peridotite xenoliths have major element chemistry different from those of selvage.

Many fluid inclusions less than 30 micrometer in diameter are present in olivine. Raman spectroscopy shows that those fluid inclusions are mainly composed of H₂O, magnesite, unidentified crystal and a bubble. Raman spectra indicate the presence of hydrous mineral on a wall of host olivine, which can be a talc. In addition to these phases, CO₂ is also found in vapor bubbles in inclusions. These suggest that the inclusions were composed of H₂O-CO₂ and reacted with olivine to form talc, magnesite, and CO₂ - bearing aqueous fluids. Using a cooling stage, we determined melting temperature of ice and estimated NaCl equivalent amount dissolved in the fluid inclusions to be 5-14 weight %. This amount of NaCl is not strictly but roughly consistent with an estimation based on Raman spectra. Since the original fluids reacted with olivine after their capture, homogenization temperature without re-reaction involved of olivine, magnesite, talc, and fluids does not provide meaningful density of original fluids.

As a pioneer work, Roedder (1965, American Mineralogist) reported CO₂ inclusions commonly observed in mantle xenoliths in worldwide. One exception was CO₂-H₂O inclusion from orthopyroxene in a peridotite xenolith of Ichinome-gata, a back-arc side in the northeast Japan arc. For last 15 years, H₂O inclusions have been reported from several peridotite xenoliths in subduction zones: from Iraya, Bataan (Schiano et al., 1995, Nature), Lihir, Papua New Guinea (McInnes et al., 2001, Earth and Planetary Science Letter) and Avacha, Kamchatka (Ishimaru and Arai, 2008, Geological Society, London, Special Publications). The present description of the fluid inclusions in the Pinatubo peridotites indicates that CO₂ bearing saline aqueous fluids are present beneath the volcanic front in Bataan arc, Philippines.

Keywords: water, fluid inclusion, carbonate, peridotite, mantle, Pinatubo volcano

SCG060-P08

Room: Convention Hall

Time: May 25 16:15-18:45

Synthetic aqueous inclusions of dehydrated fluids from hydrated minerals

Shugo Ohi^{1*}, Tetsu Kogiso¹, Akira Miyake²

¹Kyoto university HES, ²Kyoto university Science

Introduction

Deep aqueous fluids derived from subducted plate significantly affect volcanic activity in the subduction zone. Therefore, it is important to examine the chemical compositions of dehydrated fluids from hydrated minerals to grasp H₂O behavior in the subduction zone. However, quantitative estimations from material sciences for deep aqueous fluids were not discussed enough, whereas thermodynamic models were sufficiently discussed. The observation and analysis of aqueous fluids is needed to grasp deep aqueous fluids behavior in the subduction zone.

In natural samples, fluids were trapped in minerals. Purpose in present study is to trap dehydrated fluids from hydrated minerals in quartz single crystals.

Previous studies

Sterner and Bodnar (1984) made synthetic fluid inclusions by using internally heated pressure vessels. They sealed quartz crystal with micro cracks and the desired fluid composition in noble metal capsules. Synthetic fluid inclusions were formed by healing fractures in natural quartz in their study. Since then, many researchers synthesized fluids inclusions. However, no one make synthetic aqueous inclusions of dehydrated fluids from hydrated minerals.

In the meanwhile, Kogiso et al. (1997) carried out dehydration experiments on a natural amphibolite under open system conditions. They estimated the chemical composition of aqueous fluid from the gap between starting amphibolite and dehydrated charge.

In present study, we trapped dehydrated fluid from hydrated minerals in quartz by using crack healing method.

Experimental methods

Starting materials were Brazilian quartz single crystals and H₂O and Mg(OH)₂. Quartz single crystals were cut into about 1-2mm size and inclusion-free crystals were selected as starting materials. Inclusion-free quartz crystals were heated to 350 C and then, immediately upon removal from the oven, quenching in cold distilled water. After drying in a vacuum oven at 150 C overnight, inclusion-free quartz crystals were sealed with an arc-welder in Pt capsules along with other starting materials.

In the first experiment, distilled water and a quartz crystal were sealed in a Pt capsule to check crack healing and trapping fluids. In the second experiment, Mg(OH)₂ and a quartz crystal were sealed. In the third experiment, Mg(OH)₂ was sealed with quartz rapped in a Pt foil (0.0025mm in thickness) with holes (30-50 μ m in diameter) to prevent the reaction between quartz and Mg(OH)₂. Pt capsules were about the bottom portions of 5 mm long, 2mm in diameter (0.1mm in thickness). The capsules were placed into piston cylinder, solid media apparatus. Experimental conditions were 800 C, 1GPa and 3 hours. After quenching, thick thinsections (60-100 μ m in thickness) were prepared to examine with a optical microscope and a scanning electron microscope equipped with and energy dispersive X-ray spectrometer.

Results and discussions

In the observation of the first sample, fluid inclusions with 5 μ m size were in quartz crystal.

In second sample, fluid inclusions with 5-15 μ m size were observed in quartz crystal. Mg₂SiO₄ polycrystal band with 100-200 μ m thickness was observed between quartz and MgO (or Mg(OH)₂). Moreover, a few MgSiO₃ crystals were observed between quartz and Mg₂SiO₄. Therefore, the reaction between quartz and Mg(OH)₂ were undoubtedly caused during the second experiments.

In third sample, fluid inclusions with 5-15 μ m size were observed. A little amount of Mg₂SiO₄ was observed on the points where quartz was not wrapped in Pt foil. However, the reaction between quartz and Mg(OH)₂ were scarcely caused during the third experiments.

Conclusion

In present study, we trapped dehydrated fluid from hydrated minerals in quartz for the first time. However, 5-15 μ m was not enough size to estimate the chemical composition of fluid inclusions. Discovery of the experimental condition to synthesize large

fluid inclusions will lead the interpretation about fluids behavior in the subduction zone.

Keywords: fluid inclusion, dehydrated fluid, synthetic experiment, piston cylinder

SCG060-P09

Room:Convention Hall

Time:May 25 16:15-18:45

Evolution of Microstructure and Flow Properties of Fault in Neogene siliceous Mudstone

Shin-ichi Uehara^{1*}, Miki Takahashi¹

¹GSI, AIST

When we evaluate patterns of flow and mass transportation through underground space, fractures and faults in rocks cause severe uncertainties. The uncertainties are partly from those in flow properties of a single fracture or fault. The flow properties of a fault and fracture generally depend on several factors such as intact rock properties or stress conditions. It is therefore important to evaluate dependencies of flow properties through a single fault on several factors, for evaluation of their effects on flow properties of bulk rock mass.

We operated laboratory experiments to measure flow rate through a mudstone specimen during axial deformation under confining pressure, with siliceous mudstone from Koetoi and Wakkanai Neogene Formations, Horonobe, Hokkaido. Main origins of Koetoi and Wakkanai Formation (Fm.) mudstones are the same, fossil diatoms, but phases of amorphous silica are different; at the boundary between these Fms., the phase changes from Opal-A to Opal-CT. Therefore Wakkani Fm. mudstone is denser and harder than Koetoi Fm. mudstone. Japan Atomic Energy Agency (JAEA) has done detail researches relating to flow properties of rock mass at underground situation, including by drilling cores or borehole explorations down to the depth of several hundred meters to a few kilometers in this region. Previous studies indicated that in-situ flow path tends to concentrate at some locations, which seems to match with the locations of faults and fractures in Wakkanai Fm., while, in Koetoi Fm., this tendency is weak. This difference can reflect differences on characteristics of flow properties of faults. Therefore we operated laboratory experiments with these rocks and tried to examine this possibility.

We adopted a specimen arrangement similar to experiments of Takahashi (2003, JGR); we put a cylindrical mudstone specimen of 20mm in length and 20mm in diameter between cylindrical Berea sandstone specimens of 10mm in length and 20mm in diameter. The mudstone specimen is intact, but the sandstone specimens have saw-cut plane of which an angle is 30 degrees with respect to the axis of the specimen. The sandstone specimens are set at the both side of the mudstone specimen so that the saw-cut planes are on the same plane, in order to induce shear zone in the mudstone specimen when axial force is applied. The advantage of this method is that we can see if flow rate along induced shear zone, or fault, is effectively large comparing to the intact part of mudstone.

We set confining pressure and average pore pressure as 8.3 and 4.9MPa, respectively, considering the condition of a depth of approx. 500m in this region. We used distilled water as a pore fluid and operated the experiments under room temperature. We applied an axial displacement with a constant velocity, 0.2um/sec, and measured permeability of the axial direction by oscillation pore pressure method. We used specimens prepared from three locations of the drilling core of HDB 10; 43.2m, 264.0m, (Koetoi Fm.), and 385.0m (Wakkanai Fm.) in depth.

Main results of the laboratory experiments and microstructure observations are as follows. (1) Measured permeability is similar to permeability before deformation, or intact permeability, for Koetoi Fm. mudstone, while, in the case of Wakkanai Fm. mudstone, permeability increases after deformation. (2) Micro focus X-ray computed tomography images of induced shear zones indicated that the shear zone in Koetoi Fm. mudstone is compacted, while that in Wakkani Fm. mudstone is dilative and fractures are observed around the shear zone, which suggested that the shear zone may work as a conduit. The differences of shear zone flow properties in laboratory experiments between two Fms. may be related to differences in observed in-situ flow.

This research is supported by the Ministry of Economy, Trade and Industry of Japan. We express our gratitude to Dr. Niizato, JAEA, for his efforts to prepare drilling core samples from HDB 10.

Keywords: fault flow property, laboratory hydro-mechanical experiment, siliceous mudstone, Horonobe, permeability, micro focus X-ray CT

SCG060-P10

Room:Convention Hall

Time:May 25 16:15-18:45

An experimental investigation on the fluid distribution in amphibolitic lower crust

Masamichi Abe¹, Michihiko Nakamura^{1*}

¹Department of Earth Science TOHOKU Univ.

The connectivity of COH fluids in the polycrystalline aggregates of pargasite, anorthite, and those two was assessed in terms of the geometry of crystal-crystal-fluid triple junction in the synthetic rocks. All the experiments were carried out at 600 degreeC and 0.7 GPa with fluid fraction of 0.1?3%. To estimate the true dihedral angles without a sectioning effect, the effect of surface energy anisotropy was considered using the cumulative frequency curve of the apparent dihedral angle measured on cross sections.

In the anorthite?fluid systems, populations of the curved-curved (CC) type triple junction were ca. 45% irrespective of the fluid composition, whereas their median dihedral angles depend on the fluid composition; 80 degree for H₂O, 93 degree for CHO and 70 degree for 6 wt.% NaCl aqueous solution. The true CC type dihedral angles, estimated according to the theory of Laporte and Provost (2000), range from 53 to 102 degree. Since most of the dihedral angles is >60 degree in the anorthite aggregate, the intergranular fluid will not be connected as long as the fluid fraction is small. In the pargasite aggregate, the CC type was less dominant; ca. 65% of the triple junction was faceted?faceted (FF) type. It should be noted that most of the FF type were impingement grain boundary. If I assume that the true dihedral angle does not have a single value but constant probability distribution, then its range is calculated to be 28?88 degree. Assuming for simplicity that the pore geometry is equilateral triangular pyramidal, the true dihedral angle has this range when the ratio of hypotenuse to base of the pyramid is 0.7?5.6. This simple model shows that the pyramid of pore fluid in the pargasite aggregate has a finite height and will not be interconnected, because if the fluid is interconnected, its geometry approaches a tube lacking the base plane and the maximum value of the true dihedral angle (formed only with two side faces) is less than 60 degree. In the anorthite-pargasite-fluid system, the population of the triple junction consisting of a curved anorthite and a faceted pargasite faces is >65%. It is calculated that the true dihedral angle of this type of triple junction has a range of 31?57 degree on the basis of the cumulative frequency curve of the measured apparent dihedral angle.

The FE-SEM observation showed that most of the FF and FC type boundaries were formed by impingement, and thus surface tensions at these grain boundaries were not balanced. However, such boundaries were stable as long as the experimental duration. In addition, it is observed that the impingement grains are common in natural amphibole or biotite in the high-grade metamorphic rocks. Therefore, the pore geometry determined by the impingement grains seem to represent a stable structure. Judging from the observed pore-type populations, the FFC and FCC type pores are most likely in the amphibolitic aggregate. The connectivity of these types of pore are relatively high, because the FC type dihedral angle is relatively low (31 - 57 degree) even at the small fluid fraction of the present experiments and the curvature can be continuous along the curved grain boundary (von Bargen and Waff, 1986). The fluid may be interconnected along the edges surrounded by the faceted plane(s) and curved edge(s). The possibility of interconnection at the grain corners is also high. Thus, the connectivity of fluid in the aggregates of amphibole and anorthite is strongly dependent on the modal composition.

Keywords: continental lower crust, low electrical resistivity, interconnected fluid, dihedral angle, surface energy anisotropy

SCG060-P11

Room:Convention Hall

Time:May 25 16:15-18:45

Experimental study on calcite precipitation in hydrothermal environments

Michimasa Musha^{1*}

¹Tohoku Univ.

The crustal fluids are commonly characterized by the compositions in C-H-O system, mainly composed of H₂O, CO₂ and CH₄, and thus transport of these fluids and precipitation of carbonate are important for the global carbon cycle. To reduce greenhouse gas (CO₂, CH₄ etc) in the atmosphere, the carbon storage underground has been tried; however, it is considered to be difficult to precipitate calcite in reasonable timescale. In contrast, calcite veins are very common in the oceanic crusts, metamorphic rocks, and accretionary prisms. For example, calcite + quartz veins occur ubiquitously in the Shimanto belt. The solubility of calcite decreased with temperature, that is the opposite trend of quartz; and thus how calcite precipitated in the conditions that quartz also occurs is puzzling. In spite of its importance, the experimental studies on the calcite precipitation are very limited. Most experiments are carried out under near room temperature and controlled by pH change or synthetic CO₂ saturated fluids (Lee & Morse, 1999), that are far from natural conditions of calcite-vein formation. To best of our knowledge, there are no experimental studies on calcite precipitation under hydrothermal conditions (>100 degree C).

The purpose of this study is to understand the controlling factors on calcite precipitation under conditions of calcite-vein formation (fluid compositions, P-T conditions, host rock types). The solubility of calcite increases with decreasing temperature, with increasing fluid pressures, and with increasing concentration of NaCl (Ellis, 1963). What is the most controlling factor that enhances the calcite-vein formation at the conditions of the Shimanto belt is unknown. As a first step, we conducted hydrothermal flow-through experiments to precipitate calcite at 300 degree C and 30 MPa by using the temperature dependency of solubility.

Before the precipitation experiments, because a reliable solubility data on calcite at elevated temperature is lacking, we tested how amount of Ca ions dissolved from calcite in the flow-through system at 30 MPa with temperature range from 100 to 400 degree C. The Ca concentration path-through the vessel is highest at 100 degree C, and it decreased with increasing temperature.

The experimental apparatus of the precipitation experiments is composed of two reaction vessels; in the first vessel, the super-saturated solutions were prepared by dissolution of limestone sand (1-2 mm in size) in the distilled water at 100 degree C. In the second vessel, seven limestone substrates (5x5x15 mm) were set along the flow-path. The limestone is composed of fine grained aggregate of calcite (<0.03 mm). The temperature of the precipitation vessel was set to be 300 degree C. The fluid flow rate was 1 ml/min. After the run of 240 h (10 days), the total increase of weight of limestone substrates was 0.051 g. Observation of the surface morphologies of the substrates by SEM and thin sections by optical microscope reveal that euhedral calcite crystals with size of 0.02-0.03 mm grew from the calcite in the substrates.

Our results suggest that calcite veins could be formed around 300 degree C, if fluids saturated with calcite at lower temperature would be brought accompanying with subduction of slabs. However, our experimental conditions deviate from that of quartz and calcite vein formation, because the temperature increase leads to the dissolution of quartz, so that it cannot be co-existing of quartz and calcite in the same veins. Second, the source of Ca and CO₃²⁻ would be the host sedimentary or basaltic rocks in the Shimanto belt. We will try to precipitate calcite with using other factors, including pressure dependence on the solubility, the host rock type.

References: Lewis J. C., Byrne T. B., J.D.Pasteris, (2000), *J. metamorphic Geol.*, 2000, 18, 319-333

Y. J. Lee, J. W. Morse, (1999), *Chemical Geology*, 156 (1999), 151-170

A. J. Ellis, (1963), *American Journal of Science*, 261, 1963, 259-267

Keywords: accretionary prism, subduction zone, calcite, mineral veins

SCG060-P12

Room:Convention Hall

Time:May 25 16:15-18:45

Optical pressure sensors for DAC experiment: application in high-pressure studies

Nadezda Chertkova^{1*}, Shigeru Yamashita²

¹ISEI, Okayama University, ²ISEI, Okayama University

Structural properties of melts and minerals are widely examined by in situ spectroscopic studies with externally heated diamond anvil cell (HDAC) [1]. While the temperature can be controlled with an accuracy of plus/minus 0.5-1.5 degree C with this technique [2], a direct pressure measurement is complicated by the differences in compressibility and thermal expansivity for the variety of samples. Only few spectroscopic standards can be used for pressure determination in the HDAC experiments involving silicate melts. One of the non-reactive pressure sensors which was calibrated in the wide pressure- and temperature ranges is ¹³C diamond [3]. Its first-order Raman shift is distinct from that of diamond anvils and indicates the pressure in immediate proximity to the sample.

The objective of this work was to test the precision of ¹³C diamond pressure marker at high pressures and elevated temperatures. Experiments were carried out in the HDAC, with pure H₂O as a pressure medium and two optical pressure markers - ¹³C diamond aggregate chip and ruby chip. Already well established phase transitions in H₂O system and ruby fluorescence pressure scale were used as references for checking the precision of pressure determination with ¹³C diamond Raman shift.

In the temperature (22-300 degree C) and pressure (up to 4.8 GPa) ranges studied, a good agreement between the phase transitions in H₂O system and the pressure values obtained from two pressure sensors was achieved during heating cycles. The average difference between pressures calculated from ¹³C diamond Raman shift and those calculated from ruby fluorescence line shift (0.16 GPa) lies within the reported uncertainty of calibrations [3], [4], [5]. The largest full width at half-maximum (FWHM) for the first-order Raman peak of ¹³C diamond was found to be approximately 9.9 cm⁻¹ at 300 degree C, that is much smaller than FWHM for ruby fluorescence lines.

Experiments in the H₂O system demonstrated that ¹³C diamond is a precise pressure sensor which immediately detects sudden pressure drops in the case of sample decapsulation. These features are essential for the pressure control in in-situ studies of magmatic phenomena, such as mixing behavior of magma and volatiles, structural changes in melts and fluids, crystallization sequences.

References

1. Smith R.L. and Fang Zh. (2009) Techniques, applications and future prospects of diamond anvil cells for studying supercritical water systems. *Journal of Supercritical Fluids*, V. 47, P. 431-446.
2. Bassett W.A., Shen A.H., Bucknum M., and Chou I.M. (1993) A new diamond cell for hydrothermal studies to 2.5 GPa and from -190 degree C to 1200 degree C. *Reviews of Scientific Instruments*, V. 64, P. 2340-2345.
3. Schiferl D., Nicol M., Zaug J.M., Sharma S.K., Cooney T.F., Wang S.-Y., Anthony T.P., Fleischer J.F. (1997) The diamond ¹³C/¹²C isotope Raman pressure sensor system for high-temperature/pressure diamond-anvil cells with reactive samples. *Journal of Applied Physics*, V. 82, P. 3256-3265.
4. Zha C.S., Mao H.K., and Hemley R.J. (2000) Elasticity of MgO and a primary pressure scale to 55 GPa. *PNAS*, V. 97, P. 13494-13499.
5. Ragan D.D., Gustavsen R., Schiferl D. (1992) Calibration of the ruby R₁ and R₂ fluorescence shifts as a function of temperature from 0 to 600 K. *Journal of Applied Physics*, V. 72, P. 5539-5544.

Keywords: diamond anvil cell, ¹³C diamond, ruby, pressure sensor

SCG060-P13

Room:Convention Hall

Time:May 25 16:15-18:45

Seismic velocities of crustal rocks and minerals

Kyoko Matsukage^{1*}, Yu Nishihara²

¹GRC, Ehime University, ²SRFC, Ehime University

Recently, seismologists obtain high-resolution data of crust and mantle on distribution of seismic wave velocities (e.g., Nakajima et al., 2001). For interpretation the origin of distribution of seismic wave velocities, we have to know the relation between chemical variation and its seismological signature. There are two methods to obtain the relation. The first is direct seismic velocities measurement of bulk rock (multi-phases sample) by using high-pressure apparatus (e.g., Nishimoto et al. 2008; Kono et al. 2009). The second is theoretical calculation by using the data of well-defined thermoelastic parameters of minerals and modal composition. We can calculate the seismic velocities of rocks at various temperatures and pressures in the Earth's interior if some important thermoelastic parameters of constituent minerals, such as bulk modulus, its pressure derivative, density, Debye temperature, Gruneisen parameter, shear modulus and its pressure derivative at room pressure and temperature are obtained. Recently, we can obtain reliable thermoelastic parameters of upper mantle minerals by literatures in wide pressure and temperatures range, which cover the whole upper mantle of the Earth (e.g., compiled by Matsukage et al., 2005). Therefore the calculated seismic velocities of mantle rocks such as lherzolite and harzburgite can be compared directly with the seismic velocities profiles observed by seismologists (e.g. PREM, AK135).

On the other hand, the thermoelastic parameters of crustal minerals (e.g., amphibole and plagioclase) are not determined very well because of at least two experimental difficulties. The first problem is the low symmetric crystal structure of crustal minerals. The second problem is the narrow stability field, less than ~ 3 GPa and ~ 1300 K. In this study, we try to calculate the thermoelastic parameters of crustal minerals by using the P-V-T equation of state data and heat capacity measured by previous studies, and estimate the seismic velocities of gabbroic and eclogite rocks with various chemical compositions at high-pressure and high-temperature. We also try to measure the elastic wave velocities and density (P-V-T data) of plagioclase and amphibole by using the multi-anvil apparatus with synchrotron X-ray in SPring-8. In this presentation, we are going to discuss the reliability of the calculation and show the relation between chemical variation of crustal rocks and its seismological signature.

Keywords: seismic velocity, gabbro, eclogite, plagioclase, amphibole, pyroxene

SCG060-P14

Room:Convention Hall

Time:May 25 16:15-18:45

Seismic Velocity Structure beneath Kii Peninsula

Taishi Fukui^{1*}, Takuo Shibutani¹, Setsuro Nakao¹, Kazuhiro Nishimura¹, Masayo Sawada¹, Kazuro Hirahara²

¹DPRI, Kyoto Univ., ²Science, Kyoto Univ.

Philippine Sea Plate is subducting beneath the southwest Japan arc from the Nankai Trough. This causes megathrust earthquakes in the subduction zone. The latest events along the Nankai Trough are Showa Tonankai Earthquake (M7.9) in 1944 and Showa Nankai Earthquake (M8.0) in 1946. The next event is predicted to occur in 2030 - 2036 (Earthquake Research Committee, 2001). It is thought that the surrounding area of the southern edge of Kii Peninsula is most likely to be a rupture starting point of the megathrust events as it was in the Showa events. At the same time, the Kii Peninsula is a region through which hazardous seismic waves propagate from the megaquakes to large cities such as Osaka, Kyoto and Nara. The purpose of this study is to estimate structure of seismic velocity discontinuities, especially slab configurations beneath the Kii Peninsula. This is very important to upgrade the ways of predicting megaquake generations and strong motions caused by the events.

We have carried out linear array seismic observations in the Kii Peninsula since 2004. We deploy temporary seismic stations in the vicinity of profile lines with an average spacing of ~5 km and a length greater than 80 km (Fig. 1). We obtain images of seismic velocity discontinuities beneath the Kii Peninsula by using a receiver function analysis with teleseismic waveforms, and estimate structure of the subducting slab and the surrounding regions in detail. We have completed the observations and analyses for three profiles in the subduction direction (Shiono Cape - Tajiri Line AA', Shingu - Kawachi-nagano Line BB', Owase - Kyotango Line CC') so far. As a result, the upper surface of the low velocity oceanic crust (the upper surface of the Philippine Sea slab), the oceanic Moho in the slab and the continental Moho in the arc side were clearly imaged. Furthermore, strong low velocity anomalies were found in the vicinity of the slab in the generating area of the deep low frequency events and widely in the mantle wedge.

We redeployed temporary stations along three profile lines in March 2009. One is Minami-ise - Shigaraki Line DD' in the subduction direction and the others are Matsuzaka - Shirahama Line EE' and Kameyama - Gobo Line FF' in the perpendicular direction.

We estimated the depth contours for the continental Moho, the upper surface of the oceanic crust and the oceanic Moho by combining depth data of the discontinuities beneath the six survey lines picked up on the receiver function images.

In this presentation we will introduce the linear array seismic observation in the Kii Peninsula, the estimated features of the Philippine Sea slab configuration and the mantle wedge structure and the features of the contour maps of the three discontinuities.

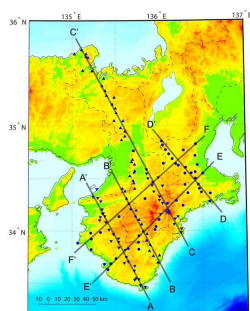


fig1. Seismic observation stations in the Kii Peninsula ▲, ●.
Survey lines(AA', BB', CC', DD', EE', FF') are solid lines in the map.

Keywords: philippine Sea slab, Mantle wedge, Receiver function image, Linear array seismic observation, Kii Peninsula

SCG060-P15

Room:Convention Hall

Time:May 25 16:15-18:45

Receiver function imaging of the Philippine Sea slab beneath Kyushu, southwest Japan

Yuki Abe^{1*}, Takahiro Ohkura¹, Kazuro Hirahara², Takuo Shibutani³

¹AVL, Kyoto Univ., ²Graduate School of Science, Kyoto Univ., ³DPRI, Kyoto Univ.

In subduction zones, the subducting slabs are thought to convey fluid into the mantle wedge and to cause arc volcanism. It is revealed that serpentinized layer in the mantle wedge beneath NE Japan subducts along the Pacific slab, releases its fluid at about 150 km in depth, and the released fluid moves to the volcanic front, with seismic tomography, receiver function (RF) analysis and geochemical simulation (Hasegawa et al., 2008; Iwamori, 2007; Kawakatsu & Watada, 2007). Oceanic plates subducting beneath Kyushu (west Philippine Sea basin: 50Ma. Shikoku basin: 27Ma) are younger than the Pacific plate subducting beneath NE Japan (130Ma), and an island arc crust, Kyushu-Palau ridge, is subducting beneath Kyushu. The mantle wedge structure beneath Kyushu has been estimated and fluid distribution has been elucidated by tomographic studies (Zhao et al., 2000; Honda & Nakanishi, 2003; Wang & Zhao, 2006). It is revealed that the subducted oceanic crust exists at 60 km in depth and the Philippine Sea slab (PHS) conveys fluid down to this depth beneath the central part of Kyushu (Okamoto et al., 2008). However, it has not been elucidated where the hydrated portion extends along PHS. It is important to estimate the structure of PHS and reveal hydrated portion for better understanding of fluid transportation by a young slab. We estimate the geometry of seismic velocity discontinuities of PHS with RF analysis.

We use 439 teleseismic waveforms (origin time: Aug.1996-Feb.2009, epicentral distance: 30-90°, magnitude: greater than 5.5) observed at 78 Hi-net stations and 61 J-array stations. Transverse RFs which hail from the southeast are constructed with the extended-time multitaper method (Shibutani et al., 2008). We use the fast-marching method (de Kool et al., 2006) to stack RFs with taking account of refraction at dipping interfaces (Abe et al., submitted). RFs are stacked in a region (31-34°N, 129-132°E and 0-300 km in depth), which includes the Wadati-Benioff zone of PHS beneath Kyushu, and projected on sections perpendicular to the strike of PHS. We assume a 1-d model of ak135 (Kennett et al., 1995), and stack RFs several times with assuming varying geometries of conversion surfaces, so that the assumed interface geometry coincides with that obtained from RF sections.

We obtain discontinuities with upward decreasing velocity along the Wadati-Benioff zone of PHS. These discontinuities extend to 80-150 km in depth. Discontinuities with upward decreasing velocity along a slab are expected to be the oceanic Moho or the bottom interfaces of serpentinized mantle (Kawakatsu & Watada, 2007). Since these obtained discontinuities extend up to 150 km, shallower and deeper portions of them are interpreted as the oceanic Moho and the bottom interfaces of serpentinized mantle, respectively, although we do not distinguish the two interfaces. Therefore, these discontinuities are expected to be the bottom of hydrated portion, and fluid transportation along PHS is revealed.

We obtain discontinuities which are interpreted as the top surface of PHS only in the region, at 32°N, 60-80 km in depth. They might be the top surface of the island arc crust (Kyushu-Palau ridge), and the structure of this region should be examined more in detail. Discontinuities interpreted as the top surface of PHS do not detected beneath the other region. This fact indicates that seismic velocity contrast at the top surface of PHS is small, and is consistent with the fact that the fore-arc mantle wedge has low seismic velocity (Zhao et al., 2000; Honda & Nakanishi, 2003; Wang & Zhao, 2006).

We use waveform data observed by the National Research Institute for Earth Science and Disaster Prevention, Kyushu Univ., Kagoshima Univ. and Japan Meteorological Agency, and hypocentral data collected by Japan Meteorological Agency. We use FMTOMO (de Kool et al., 2006) to calculate travel time fields with the fast-marching method.

Keywords: receiver function, Philippine Sea slab, Kyushu, fast-marching method

SCG060-P16

Room:Convention Hall

Time:May 25 16:15-18:45

3D electrical resistivity modeling of the Onikobe caldera -Implications for volcanoes and earthquake activity

Hiromi Fukino¹, Yasuo Ogawa^{2*}, Masahiro Ichiki³, Wataru Kanda², Bulent Tank⁴

¹EPS, Titech, ²KSV0,Titech, ³Tohoku Univ., ⁴Bogazici Univ.

The Onikobe caldera is an oval topographic depression of 7.5km x 10km. In its southern part, there are active geothermal fields in east-west directions and the most active geothermal manifestation Katayama-Jigoku is in its southeastern end. Around the area, many crustal earthquakes occur, such as Iwate-Miyagi Nairiku Earthquake(Mw 6.9). The objective of this study is to image the resistivity structure in three dimensions in order to relate the distribution of fluids to volcanoes and earthquakes.

MT survey of 30 sites was conducted in 2009 in and around the Onikobe caldera. Three-dimensional inversion (WSINV3DMT) was applied to the dataset using the full impedance components. The results of the inversions are as follows. A low resistivity body with north-south strike was found at 20km depth in the western part of the caldera. The conductor extends upward, but it starts to branch laterally at 15km depth. One minor branch goes to 3km depth under the Mukaimachi caldera, which is located to the south-west of Onikobe caldera. Another major conductive branch reaches 2km depth below the surface of Katayama-Jigoku. The latter conductor has an east-west strike, which reflects the regional direction of tectonic compression. The resistivity of such crustal anomaly is between 1 and 10 ohmm. Using the Hashin-Strikman model, where conductive fluid shells cover the resistive rock matrix, the conductors will have fluid content as 1-7%, if we assume typical saline crustal fluids. Earthquakes occur at resistive zone above conductive body. This suggests the triggering of earthquake by fluids.

Keywords: magnetotelluric, inland ?earthquake, geofluid

SCG060-P17

Room:Convention Hall

Time:May 25 16:15-18:45

The effect of heat and fluid on dynamic earthquake rupture in inhomogeneous stress field

Ryo Itoh^{1*}, Takehito Suzuki², Satoshi Ide²

¹ERI, Univ. Tokyo, ²EPS, Univ. Tokyo

We numerically investigate the effect of the interaction among heat and fluid on dynamic fault tip growth. The interaction, referred to as thermal pressurization (TP), is briefly summarized as follows. When fault slip occurs, frictional heat source appears and it raises fluid pressure. The high-pressured fluid reduces effective normal stress acting on the fault plane, which reduces the frictional stress. This frictional stress reduction enhances the fault slip and the heat source term is again changed. TP is therefore regarded as positive feedback in dynamic fault slip process. Though this mechanism has been studied widely, there has been a problem that many researchers have assumed homogeneous model setup. Natural faults show inhomogeneity in many aspects such as material properties and stress field. For example, the slab beneath Tohoku shows compression (upper zone) and tension (lower zone) stress field and earthquakes are observed to propagate in such stress field. In addition, fluid dehydrated from rocks is believed to exist in and around the slab and it is expected that TP works strongly in the region. We should therefore consider how TP works in inhomogeneous stress field.

We assume dynamic fault tip growth in a thermoporoelastic medium; thermoporoelastic medium has been assumed by a number of researchers to treat TP. Spontaneous fault tip growth with the Coulomb fracture criterion is assumed. Shear stress acting on the fault plane is assumed to decrease linearly with distance from the rupture nucleation point, which generates the region where the shear stress acts in the opposite direction. We can therefore expect that the fault tip growth is arrested spontaneously if we do not consider TP.

The fault tip with TP is found in our calculations to extend to the region where the shear stress changes its direction from the nucleation point, which occurs because of the positive feedback due to TP. If the spatial change rate of the shear stress is smaller, the fault tip can grow further. The results obtained here may explain the reason that earthquakes occurring in, for example, the Tohoku slab can extend over both compression and tension regions.

Keywords: fluid, heat, inhomogeneous stress field, slab, dynamic earthquake rupture

SCG060-P18

Room:Convention Hall

Time:May 25 16:15-18:45

Heterogeneity beneath Japan as inferred from energy partitioning of P-wave and implication for seismic radial anisotropy

Mare Yamamoto^{1*}

¹Geophysics, Science, Tohoku University

Seismic radial anisotropy is generally attributed to horizontal layering (especially with thin fluid layer and fluid-filled cracks) and/or large-scale deformation in the lower crust and upper mantle, and it has been extensively studied by surface wave analyses in order to elucidate geodynamical processes and fluid circulation. However, use of surface waves having long wavelength makes it rather difficult to discriminate between solid-fluid layering and TI anisotropy of the media. On the other hand, it is also known that the short-wavelength heterogeneity in the crust and upper mantle causes the scattering phenomena of high-frequency seismic waves such as the excitation of transverse component of teleseismic P-wave.

In this study, by systematically analyzing the excitation of transverse component of P-wave observed at NIED Hi-net stations, we map spatial variation of the heterogeneity beneath Japanese island and examine the detectability of radial anisotropy. We also compute the wave scattering in anisotropic random media using the finite difference method, and study the dependence of excitation of transverse component to the propagation direction.

In the data processing, for each frequency band, we calculate the energy partition of direct P-wave into the transverse component at each station. After averaging over events with different incident azimuthal direction and incident angle, spatial variation of the normalized transverse energy shows consistent feature with the tomographic image and spatial variation of coda-Q. This result suggests that the observation of energy partition is a good measure to characterize the structural heterogeneity. On the other hand, the normalized transverse energy also shows dependence to the incident angle, which cannot be explained by wave propagation in simple isotropic random media. To understand the cause of the angular dependence of the normalized transverse energy, we conducted finite difference modeling of the wave scattering due to anisotropic random media and examine the effects of incident angle. The results of numerical modeling indicate that the observed characteristic can be explained by oblique propagation of P wave into anisotropic random media having longer correlation distance in horizontal directions. These results imply that it may be possible to have new insight into the cause of radial anisotropy, deformation field, and fluid distribution beneath Japanese island.

Acknowledgment: I used Hi-net data provided by the National Research Institute for Earth Science and Disaster Prevention.

Keywords: Seismic wave propagation, Seismic wave scattering, Geofluid

SCG060-P19

Room:Convention Hall

Time:May 25 16:15-18:45

Estimation of corner frequency using the spectral ratio method and attenuation structure beneath NE Japan

Shuhei Hada^{1*}, Junichi Nakajima¹, Naoki Uchida¹, Erika Hayami¹, Norihito Umino¹

¹Tohoku University

Seismic attenuation is sensitive to temperature, water content, chemical composition and partial melting in a different way from that of velocity. Hada et al. (2010) estimated 3-D attenuation structure beneath northeastern (NE) Japan, using the method of Eberhart-Phillips and Chadwick (2002). In this method, spectra of waveforms from local earthquakes were used to determine simultaneously whole ray path attenuation terms, t^* , spectral level, c_0 and corner frequency, f_c . However, it is difficult to estimate accurate t^* because of a strong trade-off between t^* and f_c . Here, we estimate an exact value of f_c of each earthquake, using the spectral ratio method, and determine t^* precisely for each event-station pair.

We apply Multi-window Spectral Ratio method (Imanishi and Ellsworth, 2006) to S-wave coda, instead of direct waves, to obtain more stable spectral ratios. This method can remove the effects of a radiation pattern of source mechanism, site amplification, and heterogeneous structure. We analyzed 641 intraslab earthquakes ($M > 2.5$) beneath NE Japan for the period from 2006 to 2009. Waveforms were recorded at a nation-wide seismograph network with a sampling frequency of 100 Hz. First, spectral ratios of two earthquakes were calculated for common stations for five moving windows by overlapping half duration of each window length of 0.25s. All the calculated spectral ratios were then stacked, and f_c of each earthquake was estimated by fitting the average spectral ratio to an omega-squared source model at frequency ranges of $S/N > 3$. Finally, t^* of each event-station pair was estimated from the decay of spectrum at higher frequencies than f_c .

The obtained results show that f_c and t^* are estimated more precisely than by Hada et al. (2010). Estimated corner frequencies follow cube-root scaling with seismic moment and 0.1-10 MPa stress drop. In addition, t^* calculated for adjacent earthquakes are very similar to each other, indicating the stability of our strategy used in this study. Estimated t^* shows a prominent along-arc variation with small t^* (low attenuation) in the fore arc and high t^* (high attenuation) in the back arc, which probably reflect the difference in the nature of the mantle wedge structure. In the next step, we will perform tomographic inversion using the calculated t^* and estimate 3D seismic attenuation structure to understand ongoing subduction-zone processes in the mantle.

SCG060-P20

Room: Convention Hall

Time: May 25 16:15-18:45

Estimation of the stress field and the pore-pressure from focal mechanisms in the focal area of the 2008 IMNE

Keisuke Yoshida¹, Tomomi Okada¹, Yoshihiro Ito^{1*}, Takeshi Inuma¹, Norihito Umino¹, Akira Hasegawa¹, Group for the after-shock observations of the Iwate-Miyagi Nairiku Earthquake²

¹RCPEV, ²GIMNE2008

1. Introduction

The 2008 Iwate Miyagi Nairiku earthquake with a magnitude of 7.2 occurred in the southwest part of Iwate Prefecture and northwest part of Miyagi Prefecture on June 14, 2008. Previous studies have revealed the aftershock distribution, coseismic and afterslip distribution, and seismic wave velocity structure. These studies suggest that crustal fluid may had influence of the occurrence of the mainshock.

In this study, we estimated the stress field before and after the mainshock, and pore-pressure distribution after the mainshock using the data recorded by the routine stations of Tohoku University, JMA, Hi-net-NIED, and temporal stations by the Japan Nuclear Energy Safety Organization and the Group for the aftershock observations of the Iwate-Miyagi Nairiku Earthquake in 2008.

2. Estimation of the stress field

First, we divided the data set into into 2 subsets before (1998-2008/6/14) and after the mainshock (2008/6/14-9/30), and we estimated the stress field by the stress tensor inversion (Abers and Gephart, 2001) using first motions of the earthquakes. Before the mainshock, the maximum principal stress (σ_1) direction seems to orient ESE-WNW or E-W. σ_1 -direction seems to orient E-W especially in the south of the focal area. These directions are consisted with the average directions of the P-axis of the focal mechanisms of the earthquakes in each area before the mainshock. The minimum principal stress (σ_3) axes are horizontal in the east areas, but perpendicular in the west areas. These directions are consisted with the directions of the principal strain rate in each area. (Miura et al., 2004)

After the mainshock, stress field have some varieties in the local scale (5-10km) in the focal areas. σ_1 direction are NW - SE in the east areas, but NE - SW in the shallow part (0-2 km) of west areas, and E-W in the south areas. These directions are consisted with the average directions of the P-axis of the focal mechanisms of the earthquakes in each area after the mainshock. Other areas have WNW-ESE directions of σ_1 axis. These change of the σ_1 directions before and after the mainshock can be explained by the stress change caused by the mainshock slip if we assume the low values of the deviatoric stress ($(\sigma_1 - \sigma_3) / \sigma_3 \sim 1.025$).

3. Estimation of the spatial distribution of the pore pressure

By assuming that the weakening of the frictional strength is caused by the pore-pressure, we estimated the frictional strength (Rivera and Kanamori, 2004) and the pore-pressure distribution by using the aftershock data. High pore-pressure is estimated in the western and northern parts of the focal area. S wave velocity is low beneath these high pore-pressure areas (Okada et al., 2009, 2011). The region of the high pore-pressure zone is also consisted with the spatial extent of the large coseismic and after slip (Inuma et al., 2009). These consistencies may suggest that the overpressurized fluid from the deeper part is redistributed due to the fault slip and weaken the frictional strength of the fault plane in the west area of the focal areas.

Keywords: focal mechanism, stress, pore pressure